MRDC41007.21SA

TEMPERATURE COMPENSATED PIEZOELECTRIC MATERIALS

Semi-Annual Technical Report No. 4
For Period 05/15/81 through 11/30/81

January, 1982

ARPA Order No.	3570
Program Code:	8D10
Name of Contractor:	Rockwell International Corporation
Effective Date of Contract:	May 15, 1978
Contract Expiration Date:	May 14, 1982
Amount of Contract Dollars:	$944,318
Contract Number:	F49620-78-C-0093
Principal Investigators:	Dr. R. R. Neurgaonkar (805) 498-4545, ext. 109 Dr. L. E. Cross Pennsylvania State University (814) 865-1181

Sponsored by

Advanced Research Projects Agency (DoD)
ARPA Order No. 3570
Monitored by AFOSR Under Contract No. F49620-78-C-0093

UNCLASSIFIED

SECURITY CLASSIFICATION OF THIS PAGE (When Data Entered)

REPORT DOCUMENTATION PAGE		READ INSTRUCTIONS BEFORE COMPLETING FORM
1. REPORT NUMBER **AFOSR-TR- 82 0069**	2. GOVT ACCESSION NO.	3. RECIPIENT'S CATALOG NUMBER
4. TITLE (and Subtitle) Temperature Compensated Piezoelectric Materials		5. TYPE OF REPORT & PERIOD COVERED Semi-Annual Technical Report 05/15/81 through 11/30/81
		6. PERFORMING ORG. REPORT NUMBER MRDC41007.21SA
7. AUTHOR(s) R. R. Neurgaonkar		8. CONTRACT OR GRANT NUMBER(s) F49620-78-C-0093
9. PERFORMING ORGANIZATION NAME AND ADDRESS Rockwell International Microelectronics Research and Development Center 1049 Camino Dos Rios, Thousand Oaks, CA 91360		10. PROGRAM ELEMENT, PROJECT, TASK AREA & WORK UNIT NUMBERS 61102F 3S-70/01
11. CONTROLLING OFFICE NAME AND ADDRESS Air Force Office of Scientific Research Bolling Air Force Base Washington, D.C. 20332		12. REPORT DATE January, 1982
		13. NUMBER OF PAGES 46
14. MONITORING AGENCY NAME & ADDRESS(if different from Controlling Office)		15. SECURITY CLASS. (of this report) Unclassified
		15a. DECLASSIFICATION/ DOWNGRADING SCHEDULE

16. DISTRIBUTION STATEMENT (of this Report)

Approved for public release; distribution unlimited.

17. DISTRIBUTION STATEMENT (of the abstract entered in Block 20, if different from Report)

18. SUPPLEMENTARY NOTES

19. KEY WORDS (Continue on reverse side if necessary and identify by block number)

Strontium barium niobates
Liquid phase epitaxy
Czochralski growth technique
Gibb's energy functions
Phenomenological model
Elastic compliances

20. ABSTRACT (Continue on reverse side if necessary and identify by block number)

From the electrostriction measurements on SBN crystals, it was found that the fourth order electrostrictive coupling terms are not adequate to fully describe the paraelectric phase above Curie temperature, and hence six rank coupling terms are needed; the electrostrictive coupling terms do not change markedly with cation substitution. Results of SAW measurements on the SBN:60 crystal showed that this composition possesses temperature-compensated orientations and it is similar to other best-known bronze composition PKN. Efforts are being made to establish acoustical losses correctly for this—

DD FORM 1 JAN 73 1473 EDITION OF 1 NOV 65 IS OBSOLETE

UNCLASSIFIED

SECURITY CLASSIFICATION OF THIS PAGE (When Data Entered)

composition and based on this information, necessary changes in crystal composition will be made. The liquid phase epitaxial growth work has been shown to be successful not only for the $Sr_{.5}Ba_{.5}Nb_2O_6$, but other important bronze composition $Sr_2KNb_5O_{15}$ (hetero-epitaxial growth) onto the various orientations of the SBN crystal. Efforts are under way to establish their piezoelectric and acoustical properties.

$Sr_{.5}Ba_{.5}Nb_2O_6$

TABLE OF CONTENTS

LIST OF ILLUSTRATIONS

LIST OF TABLES

1.0 PROGRESS AND TECHNICAL SUMMARY

The phenomenological model work on the $Sr_{.6}Ba_{.4}Nb_2O_6$ single crystal was continued and the thermodynamic calculations for this composition have given confidence in the applicability of the method, and of the importance of the higher order electrostriction in controlling the temperature dependence of compliances in the ferroelectric self-polarized phase. Our most urgent task was to extend the model calculations to at least two other bronze compositions so as to determine if the higher order constants are largely independent of cation make-up in the bronze family. This verification will enable us to go ahead with confidence to calculate the full gamut of elasto-dielectric properties available in the whole complex bronze structure family. To this end, our work over the last six months has been concentrated upon the growth, characterization and measurements of single crystals at selected compositions in the $(Na_xK_{1-x})_2(Sr_{1-y}Ba_y)_4Nb_{10}O_{30}$ and $Pb_{1-x}Ba_xNb_2O_6$ bronze systems.

The SAW measurement work on SBN:60 composition is in progress to establish the acoustical losses, so that it will be possible to identify the problems associated with this crystal. However, the results of the present work show that the other acoustical properties of SBN:60 are comparable with the best known bronze composition $Pb_2KNb_5O_{15}$.

The $Sr_{.5}Ba_{.5}Nb_2O_6$ and $Sr_2KNb_5O_{15}$ tungsten bronze films have successfully been grown onto the $Sr_{.6}Ba_{.4}Nb_2O_6$-substrates by the liquid phase epitaxial (LPE) technique from the BaV_2O_6 and KVO_3 solvents, respectively. The growth of these bronze compositions was studied on different crystallographically-oriented SBN substrates and it has been shown that the growth is much faster on the (001)-plate. The quality of the films is reasonably good, and films as thick as 20-60 μm have successfully been developed for acoustical and electro-optical characterization. The hetero-epitaxial growth of $Sr_2KNb_5O_{15}$ on the SBN:60-substrate has been reported for the first time and this opens a new interest in this family for their applications in a variety of areas including SAW, electro-optic, acousto-optic and non-linear optics. For the

ferroelectric films, it is important that the film is poled before they are used for characterization; this task has been accomplished successfully and we do not consider poling to be a major problem in the present work. The piezoelectric coefficients, d_{33}, d_{15}, e_{33} and e_{15}, and electromechanical coupling coefficients k_{33} and k_{15}, which are important in the present study, are evaluated. Once this task is completed, it is planned to examine their acoustical properties. Based on these results, the necessary changes in compositions will be made to obtain optimum SAW properties.

A comparative study of crystal chemistry of ferroelectric tungsten bronze $PbNb_2O_6$ was carried out. The limit of stability of the $PbNb_2O_6$ structure, specifically the orthorhombic:tetragonal structural transition and the T_c appears to be controlled primarily by the size of substitutional ions. Several compositions based on the $Pb_{1-2x}K_xLa_xNb_2O_6$ and $Pb_{1-2x}K_xBi_xNb_2O_6$ systems exhibit excellent dielectric, piezoelectric and electromechanical coupling constants and seem to be promising candidates for SAW and other device applications.

A crystal of $Sr_{.6}Ba_{.4}Nb_2O_6$ supplied by Rockwell was optically evaluated at several laboratories (Rockwell and NRL). The results of these investigations showed that SBN:60 single crystals had better optical properties than $LiNbO_3$ and $LiTaO_3$; however, the striations seem to be somewhat a problem in the present crystals. Efforts are under way to improve the growth technique, so that it will be possible to reduce the striation problem to a degree such that the crystal can be used for optical applications.

2.0 MODELING STUDIES

2.1 Introduction

As discussed in previous reports, the thermodynamic model calculations for the $Ba_{.39}Sr_{.61}Nb_2O_6$ bronze have given confidence in the applicability of the method, and of the importance of the higher order electrostriction in controlling the temperature dependence of compliances in the ferroelectric self-polarized phase. Our most urgent task was to extend the model calculations to at least two other bronze compositions so as to determine if the higher order constants are largely independent of cation make-up in the bronze. This verification will enable us to go ahead with confidence to calculate the full gamut of elasto-dielectric properties available in the whole complex bronze structure family.

To this end, our work over the last six months has been concentrated upon the growth, characterization and measurement of single crystals at selected compositions in the $(Na_xK_{1-x})_2(Sr_{1-y}Ba_y)_4Nb_{10}O_{30}$ and $Pb_{1-x}Ba_xNb_2O_6$ families.

2.2 Selection of New Bronze Compositions

The reasoning behind the selection of the two bronze families delineated above for new model studies were as follows:

1. In the $(Na_xK_{1-x})_2(Sr_{1-y}Ba_y)_4Nb_{10}O_{30}$
   a. At the 2/4 ratio chosen, the valence is such that all the larger A_1 and A_2 sites must be filled. Thus, the ratios x and y may be modified without changing fractional occupation of A_1 or A_2.
   b. There is some evidence that fully stuffed structures of this type may have lower dielectric and elastic losses.
   c. The domain structure in this crystal can now be readily revealed by etching.

2. The $Pb_{1-x}Ba_xNb_2O_6$ family
   a. The morphotropic boundary occuring at compositions near x = 0.4 suggests that the relative stability of ferroelectric ordering along and orthogonal to the 4-fold axis is sensitive to the x value.
   b. If θ_1 is a continuously changing function of (1-x), then it should be possible to find crystals with very high e_{11} and d_{15} in this family.
   c. By combining compositions in the two families, we should be able to design materials in which we can choose the values of θ_1 and θ_3, the most important parameters in the Gibbs function.

2.3 Progress

2.3.1 Crystal Growth

Czochralski growth of crystals in both systems was carried out in a Crystalox Model MCGS3 Materials Preparation System at Penn State.

In the sodium potassium/barium strontium family, only the $K_{.2}Na_{.2}Sr_{.6}Ba_{.2}Nb_2O_6$ could be grown with all A_1 and A_2 sites filled. Other compositions which were attempted led to materials

$$K_{.12}Na_{.14}Sr_{.33}Ba_{.54}Nb_2O_6$$
$$K_{.14}Na_{.14}Sr_{.53}Ba_{.33}Nb_2O_6$$
$$K_{.13}Na_{.13}Sr_{.65}Ba_{.23}Nb_2O_6$$
$$K_{.14}Na_{.11}Sr_{.73}Ba_{.14}Nb_2O_6.$$

In each case, the composition was determined directly by chemical analysis of the crystal boule. Following a suggestion from Dr. M. Liu at Honeywell, the effect of Nd^{3+} as a growth promoter was explored in the composition $Nd_{.06}K_{.14}Na_{.12}Sr_{.48}Ba_{.30}Nb_2O_6$.

In the $Pb_{1-x}Ba_xNb_2O_6$, crystals of a size suitable for initial elasto-dielectric characterization have been grown at the compositions x = 0.7 and x = 0.5. For the $Pb_{.3}Ba_{.7}Nb_2O_6$ composition, the crystal can be grown from stoichiometric starting mixture. At the higher lead proportions, there is significant loss of PbO from the growth crucible during pulling, and melts with excess PbO are used. Composition of the pulled crystal is then determined by chemical analysis.

2.3.2 Initial Characterization

Room temperature data for the compositions $K_{.2}Na_{.2}Sr_{.6}Ba_{.2}Nb_2O_6$, $Pb_{.32}Ba_{.7}Nb_{1.99}O_3$ and $Pb_{.49}Ba_{.45}Nb_{2.1}O_6$ are given in Table 1 below. Dielectric permittivity as a function of temperature for the sodium potassium composition is given in Fig. 1, and corresponding data for the lead barium compositions in Figs. 2-5.

The good quality of the individual crystals is altered by the sharp high maxima in e_3 at T_c in each case.

In the lead-containing compositions, it is gratifying to note the enhancement of e_{11} which is occurring with increasing lead content. By taking the reciprocal of e_{11} above T_c, the Curie Weiss behavior for e_{11} is confirmed with the value of the Curie Weiss temperature θ_1 increasing from 172°K in the $PBN_{30:70}$ composition to 483°K in the $PBN_{50:50}$ composition. It was somewhat surprising to find a rather similar escalation of the transverse permittivity $_{11}$ in the KNa-containing bronze, in spite of the higher Curie point at 175°C. Again, it is satisfactory to note that the higher transverse susceptibility is accompanied by much larger values of d_{15} ~-118 and of coupling coefficient k_{15} ~37%.

Measurements are now proceeding to determine the full family of elastic, dielectric and piezoelectric constants to fit with the predictions of the thermodynamic theory.

TABLE 1

Tungsten Bronze Compounds

Property	$K_{.2}Na_{.2}Sr_{.6}Ba_{.2}Nb_2O_6$	$Pb_{.32}Ba_{.7}Nb_{1.99}O_6$	$Pb_{.49}Ba_{.45}Nb_{2.1}O_6$
Structure	Tetragonal	Tetragonal	Tetragonal
T_c (°C)	175	340	260
Lattice Constants (Å)	a_o = 12.4799 c_o = 3.9471	12.51 3.97	12.4925 3.9844
Density (g/cc)	5.16		5.93
Spontaneous polarization P_s (c/m^2) c/m^2 °K	0.30	0.40	
Pyroelectric coef. c/m^2° K	4.3×10^{-4}	1.8×10^{-4}	0.9×10^{-4}
Dielectric constants k_1	~600	360	600
k_3	~190	135	130
Piezoelectric coef. ($\times 10^{-12}$C/N)			
d_{15}	-118		
d_{31}	-28		
d_{33}	75	60	45
Piezoelectric coupl. coefficients (%)			
k_{15}	37		
k_{31}	18	14.9	
k_{33}	49		
k_p	29		
k_t	41		

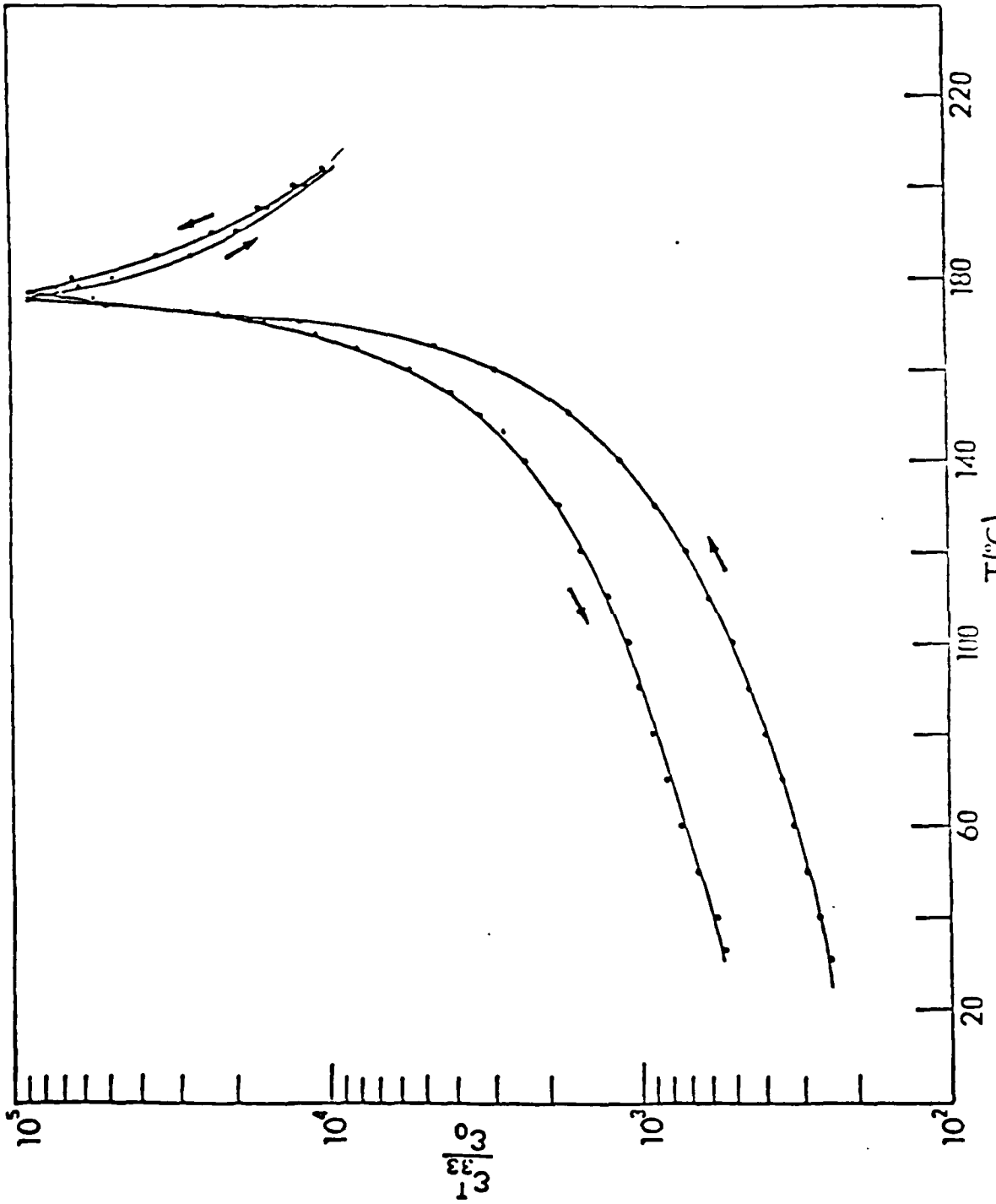

Fig. 1. Relative permittivity k^T_{33} as function of temperature in $(K_{.2}Na_{.2})(Sr_{.6}Ba_{.2})Nb_2O_6$.

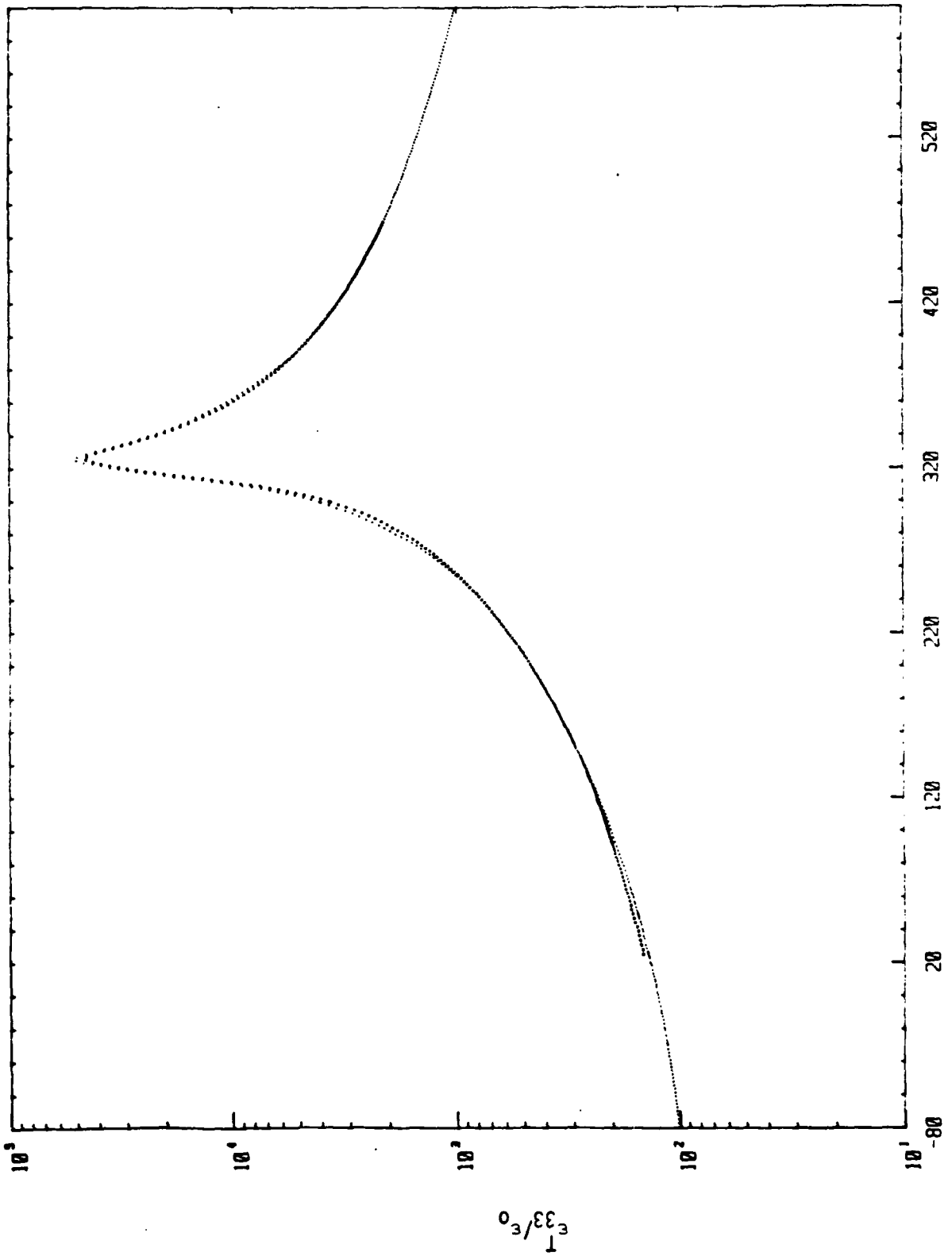

Fig. 2. Relative permittivity k_{33}^T as function of temperature in $Pb_{.3}Ba_{.7}Nb_2O_6$.

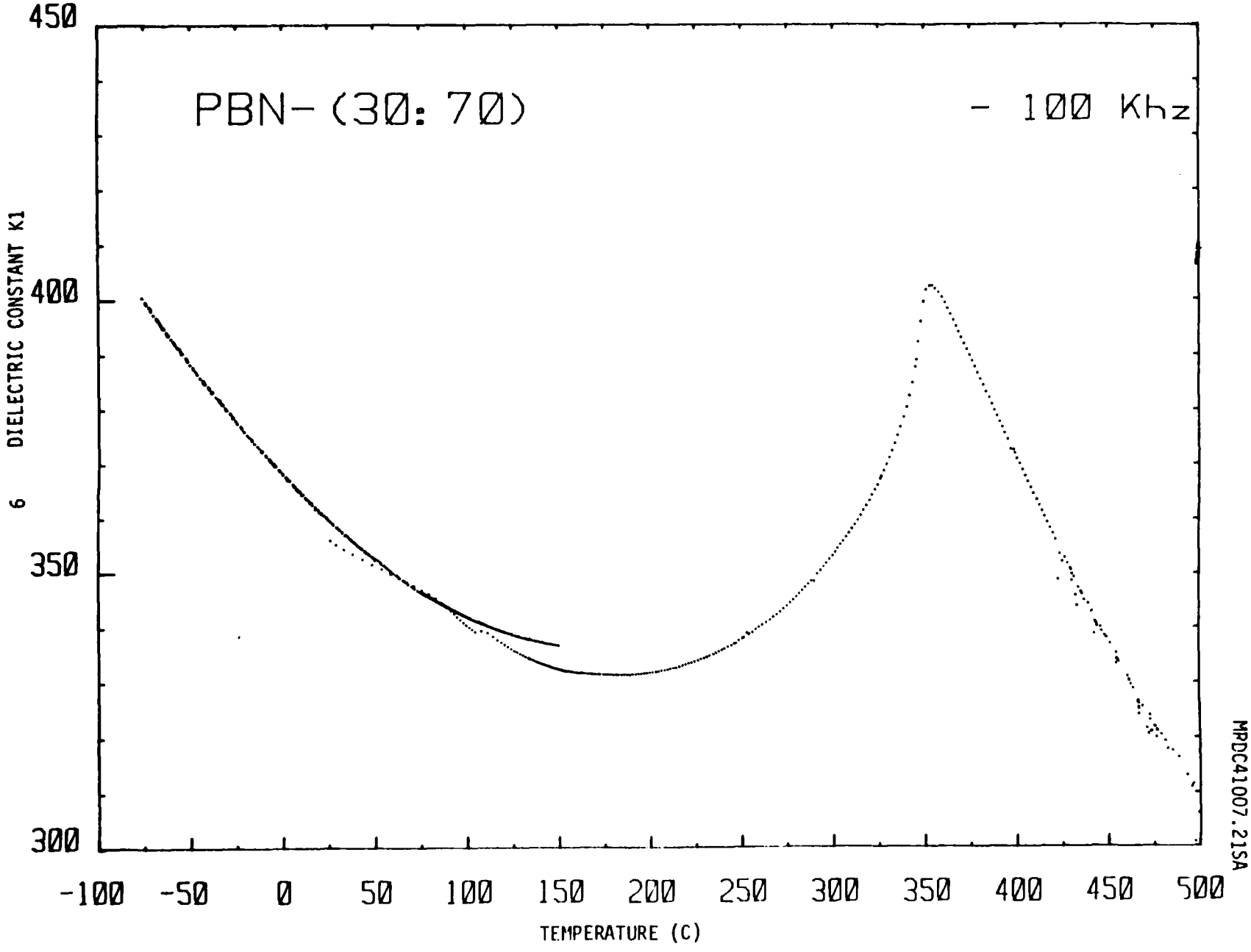

Fig. 3. Relative permittivity k_{11} as function of temperature in $Pb_{.3}Ba_{.7}Nb_2O_6$.

Rockwell International

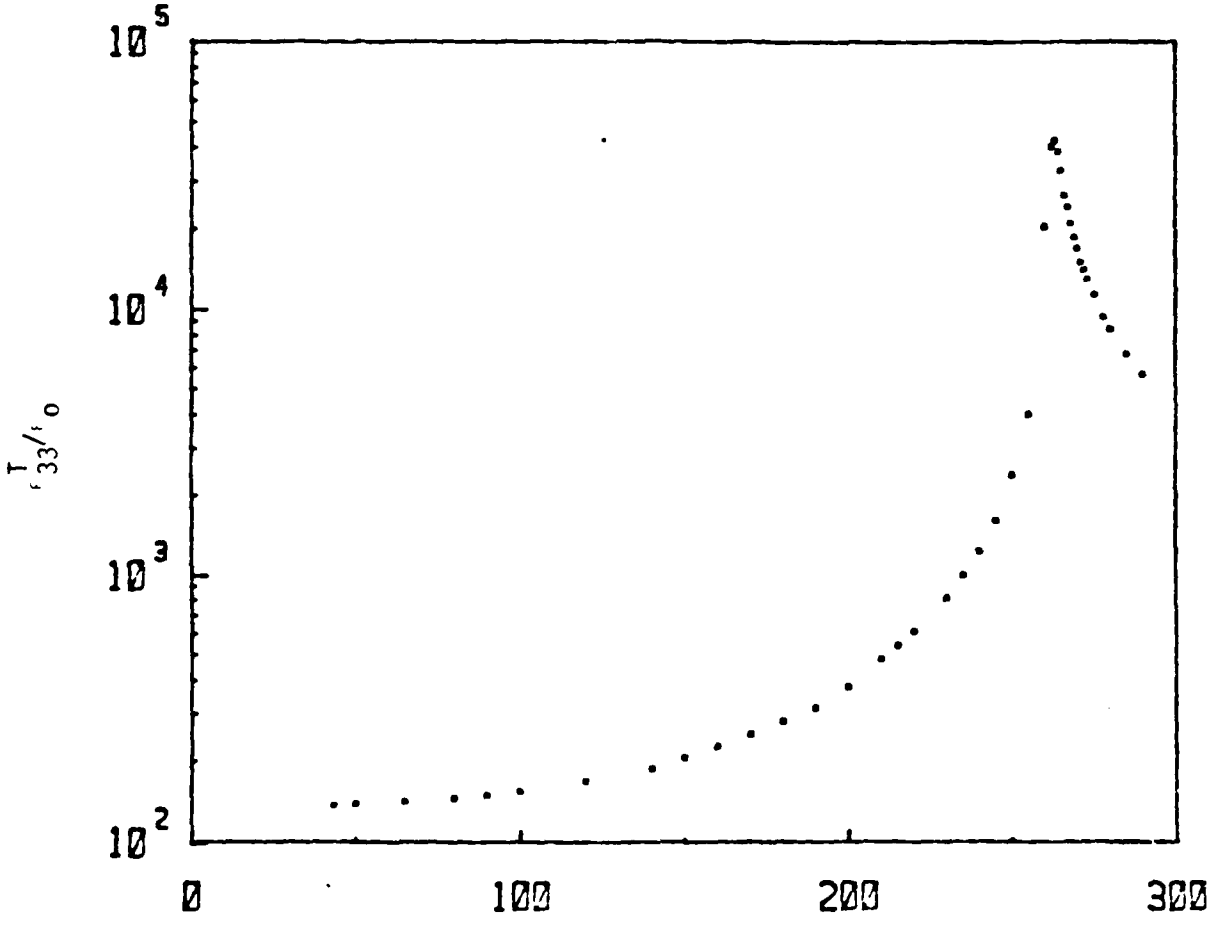

Fig. 4. Relative permittivity k^T_{33} as function of temperature in $Pb_{.5}Ba_{.5}Nb_2O_6$.

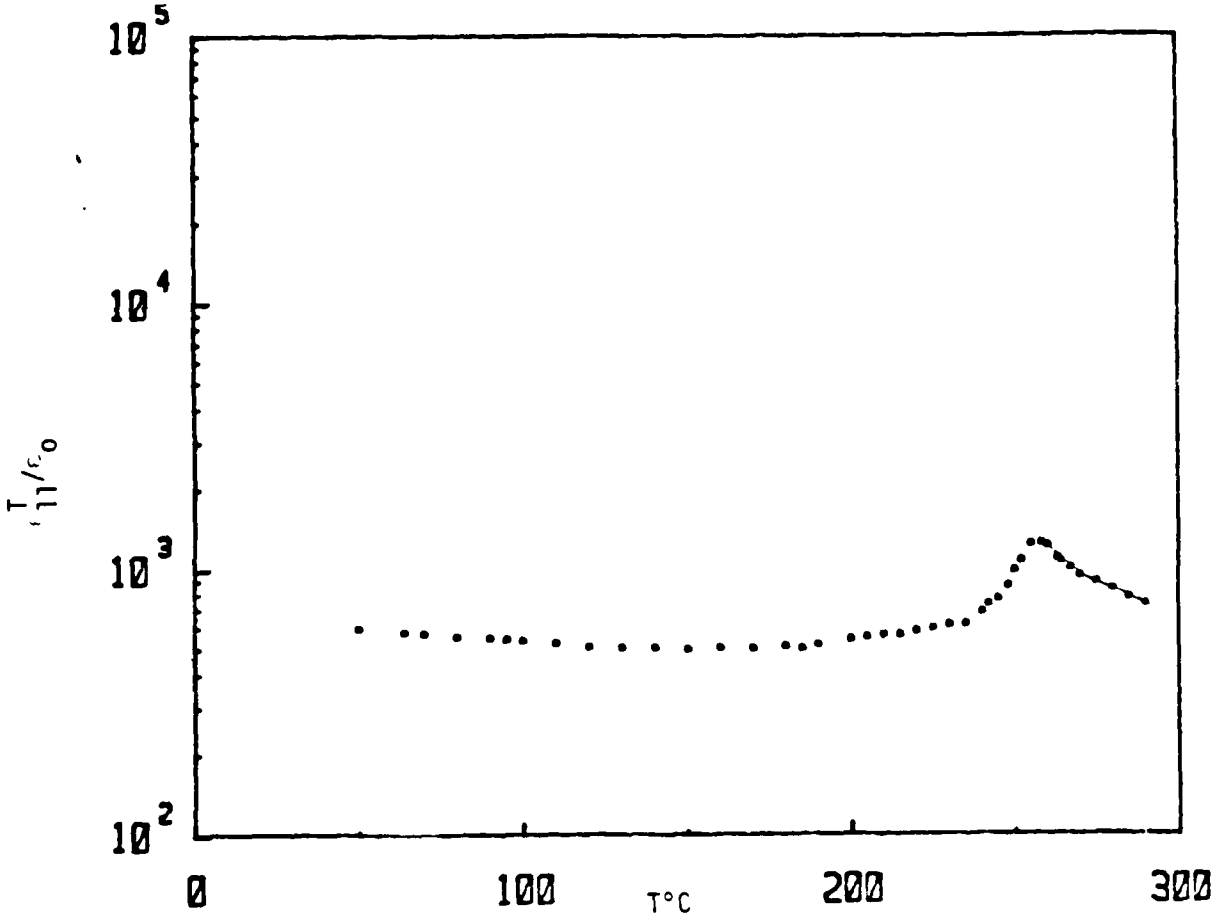

Fig. 5. Relative permittivity k_{11}^T as function of temperature in $Pb_{.5}Ba_{.5}Nb_2O_6$.

3.0 SURFACE ACOUSTIC WAVE (SAW) PROPERTIES

3.1 Introduction

The purpose of the present investigation is to develop suitable temperature-compensated tetragonal tungsten bronze compositions that possess high SAW electromechanical coupling coefficient (K^2) with a sufficiently low temperature coefficient of SAW velocity. Since the tungsten bronze structural family embraces some 100 or more known compounds and several solid solution systems, the possibility of developing a suitable composition for SAW application is very significant. Bronze compositions such as $PbKNb_5O_{15}$ (PKN), $Ba_2NaNb_5O_{15}$ (BNN), etc., have been proved to possess very attractive characteristics for SAW device applications, but these compositions did not find commercial use due to extreme difficulty in obtaining suitable size single crystals. It is then natural to trade-off some of the properties for crystals which can easily be grown and modified according to device requirements. The tetragonal bronze $Sr_{1-x}Ba_xNb_2O_6$ solid solution was selected for this study because its piezoelectric properties and Curie temperature can be changed in the desired range. Although the values k_{15} (electromechanical coupling) and d_{15} (piezoelectric constant) for SBN are much smaller than those attainable in the best bronze compositions, SBN provides a model system for studying the composition dependence of the key quantities, and for verifying the predictive power of the phenomenological Devonshire theory for these systems. The present SBN:60 single crystals not only have provided such information, but this crystal can also be used as substrate material for other SBN and bronze compositions. This is a unique advantage in the present work and makes it possible to develop other interesting and desired bronze compositions for SAW device applications. Based on our phenomenological model, other bronze compositions such as $Pb_{1-x}Ba_xNb_2O_6$ and $Ba_{2-x}Sr_xK_{1-y}Na_yNb_5O_{15}$ are potentially important since they exhibit high electromechanical coupling coefficient k_{15} and piezoelectric constant d_{15} similar to PKN. Table 2 summarizes physical

TABLE 2. Important piezoelectric tungsten bronze compositions for SAW applications.

PROPERTY	$Pb_2KNb_5O_{15}$ (PKN)	$Ba_2NaNb_5O_{15}$ (BNN)	$Sr_{.6}Ba_{.4}Nb_2O_6$ (SBN)	$K_3Li_2Nb_5O_{15}$ (KLN)	$Sr_2KNb_5O_{15}$ (SKN)	$Pb_{1-x}BaNb_2O_6$ (PBN)
Electromechanical Coupling Constant k_{33} k_{15} k_{24}	---- 0.69 0.73	0.45 0.12 0.25	0.45 0.24 ----	0.52 0.34 ----	0.45 0.30 ----	---- ---- ----
Piezoelectric Constant (10^{-12}C/N)	d_{33} = 62 d_{15} = 470 d_{24} = 470	d_{15} = 32 d_{24} = 45	d_{33} = 130 d_{15} = 31	d_{33} = 57 d_{15} = 68		d_{33} = 100 d_{15} = 200
SAW-Electromechanical Coupling Constant (K^2)	188 x 10^{-4}	----	180 x 10^{-4}	----	----	----
Temperature Coefficient of SAW Velocity	Y-cut,+24 ppm Z-cut,-30 ppm	Close to α-quartz	Z-cut,-50 ppm (110),-18 ppm	----	----	----
Curie Temperature (°C)	460	560	72	405	156	350
Crystal Symmetry	Ortho T.B.*	Ortho T.B.	Tetra T.B.	Tetra T.B.	Tetra T.B.	Tetra T.B.
References (by no.)	2-3	4	5	6		7

*T. B. = Tungsten Bronze Structure

properties for various bronze compositions. The results of the present SAW measurements have briefly been summarized in the following section.

3.2 Acoustical Characterization of SBN:60 Single Crystal

The Czochralski single crystal growth technique has successfully been developed for the congruent melting composition $Sr_{.6}Ba_{.4}Nb_2O_6$. Detailed information on the compositional boundary conditions and phase diagram have already been discussed in our earlier reports. During the past eight months, considerable effort has been made in evaluating the acoustical characteristics of the SBN:60 single crystals; this work is progressing as planned. The results are briefly discussed with our future plans and efforts in this direction.

As summarized in Table 3, surface acoustical measurements were performed on three different cuts, namely (100), (110) and (001) of the SBN:60 crystal. For the X and (110) cuts, propagation was along the (001) direction; for the Z-cut, propagation was along the (100) direction. Fifteen finger pair transducers were used, and periodicity was 104.4 μm. Transducer electrodes were photolithographically fabricated from aluminum films, approximately 1000Å thick, by conventional wet etching techniques. The detailed experimental procedure has been presented in our previous report. Results of this work showed that the tetragonal tungsten bronze composition SBN:60 possesses temperature-compensated orientations and that it appears to be suitable for SAW device applications with some minor modifications in its present acoustical characteristics. THe SAW electromechanical coupling (K^2) for three different cuts, (100), (110) and (001), of SBN:60 bulk single crystal has been established. This constant has been shown to be larger for the (001) plate propagating along the (100) direction and, as summarized in Table 3, its value is measured to be 180×10^{-4}. This value is much smaller than the best known piezoelectric Y-Z cut $LiNbO_3$ bulk single crystal (480×10^{-4}), but it is similar to the best known bronze composition $Pb_2KNb_5O_{15}$ (188×10^{-4}). The measurements on the other cuts such as (100) and (110) plates and propagating along the (001) direction were 55×10^{-4} and 60×10^{-4}, respectively. The temperature coeffi-

Table 3: ACOUSTICAL CHARACTERISTICS OF THE SBN:60 SINGLE CRYSTALS

Crystal Composition	SAW-Electromechanical coupling constant ($_K2$)	SAW-Velocity m/sec.	Acoustical Losses**		Temp. Coeff. of SAW-Velocity, at room Temperature
			Insertion	Attenuation	
SBN:60-(001) Plate Propogating along the 100 direction	180×10^{-4}	3300	17.4 dB	5.3 dB/cm	- 50 to -140 ppm/
SBN:60-(100) Plate* Propogating along the 001 direction	55×10^{-4}	3193	25.4 dB	0.8 dB/cm	
SBN:60-(110) Plate	60×10^{-4}	3173	23.7 dB	8.5 dB/cm	- 18 ppm

* A zero temperature coefficient of SAW velocity was observed for this cut at + 10°C

** All acoustical measurement were performed at 30.5 MH_z

cient of SAW velocity and acoustical losses for this composition have also been determined; these are given in Table 3. It is interesting to note that both the orthorhombic PKN and the tetragonal SBN crystals exhibit similar acoustical characteristics, even though their piezoelectric properties are different; specifically, the coupling constant k_{15} = 0.69 and the piezoelectric constant d_{15} = 470 are substantially larger for PKN than for SBN or any other bronze compositions. The PKN crystal also shows anomalous elastic constant temperature coefficients, which lead to the existance of ZTCD-cuts for SAWs. These cuts possess values of K^2_s up to 188 x 10^{-4}, while their time-bandwidth products are 0.6 x 10^{-4} sm^{-1}, which are similar to those given for $LiNbO_3$. This makes PKN very promising for SAW device application; however, this crystal did not find commercial use because of extreme difficulty in obtaining suitable size crystals for such applications. On the other hand, the bulk single crystal growth of the temperature compensated SBN:60 composition (one inch in diameter) has successfully been shown by the present authors, and as such, there is possibility that this composition can be used with some modification or it can be used as substrate material for other suitable compositions which exhibit desired acoustical characteristics. The latter approach, LPE, has already proven successful not only for the SBN:50 composition, but for other compositions such as $Sr_2KNb_5O_{15}$ (hetero-epitaxial growth).

As summarized in Table 3, the insertion and attenuation losses for the SBN:60 single crystal have also been established, and they appear to be substantially higher for the SBN:60 crystal than for other important piezoelectric materials such as $LiNbO_3$, $LiTaO_3$, PKN, etc. Similar SAW measurements on the other bronze compositions SBN:50 and SBN:75 within the $Sr_{1-x}Ba_xNb_2O_6$ solid solution system have been made by Uchica et al.[1], and their results show that these losses (for SBN:50, insertion loss 5 dB, attenuation loss 0.2 dB/cm) for the other two compositions are considerably lower order than the SBN:60 crystals. Since the SBN:60 composition is located between the other two compositions in the $SrNb_2O_6$-$BaNb_2O_6$ binary system, it was expected that these losses should be of the same order for the SBN:60 composition. In order to establish this result more conclusively, efforts are being made to determine these measurements on various other boules developed under the

present program, so that it will be possible to control the factors affecting stability, which may be associated with material growth or materials characteristics or with acoustical measurements techniques and their interpretation. Since the SBN:60 composition melts congruently in the binary system $SrNb_2O_6$-$BaNb_2O_6$, it is expected that the quality of the SBN:60 crystal should be better than any other composition within the $Sr_{1-x}Ba_xNb_2O_6$ solid solution range. However, we have already developed the SBN:60 single crystals from the melt containing ultra-pure starting materials which will produce crystals of high quality. At present, the SAW measurements are in progress on these crystals and results should be available soon. Improvements in our SAW technique are also being made in order to check the possible source of error; this should make it possible to establish correct information on these crystals.

Besides the SBN:60 single crystal, SAW measurements on the other important bronze compositions such as $Sr_{.5}Ba_{.5}Nb_2O_6$, $Sr_2KNb_5O_{15}$, $Pb_{1-x}Ba_xNb_2O_6$, $Ba_{2-x}Sr_xK_{1-y}Na_yNb_5O_{15}$, etc. have also been initiated. As summarized in Table 3, the coupling constant k_{15} and the piezoelectric constant d_{15} are significantly higher, specifically for the $Pb_{1-x}Ba_xNb_2O_6$ solid solution system, and based on our phenomenological model developed for this tungsten bronze family such compositions should exhibit interesting acoustical properties with minimum insertion as well as attenuation losses. The preliminary bulk single crystal growth work on these compositions (at Rockwell and Penn State) has already shown that small size crystals, approximately 5-10 mm in diameter, can be grown for piezoelectric characterization. During the next six months, efforts will be extended at Rockwell to develop this technique to produce the crystals of good quality and of approximately 1 to 2 cm in diameter, so that the piezoelectric as well as acoustical properties can be established to determine the optimum bronze compositions for SAW device applications.

4.0 LIQUID PHASE EPITAXIAL GROWTH OF TUNGSTEN BRONZE FAMILY COMPOSITIONS

The purpose of the liquid phase epitaxial (LPE) growth work is to develop and modify suitable tungsten bronze compositions that possess high SAW electromechanical coupling constants (K^2) with sufficient low temperature coefficient of SAW velocity. The ability of LPE to obtain a wide variety of films in a relatively short time, compared with the time required to achieve suitable quality in bulk single crystals, will enable us to greatly expand our knowledge of obtainable properties in this class of materials. Since large size single crystals of bronze compositions $Sr_{1-x}Ba_xNb_2O_6$, where x = 0.60 and 0.50, are now available from our current work and, secondly, since the LPE growth of $Sr_{.5}Ba_{.5}Nb_2O_6$ has been shown to be successful[5], this approach seems to be most exciting in the present work to develop either simple or complex bronze compositions for SAW device applications. It is interesting to note that the bronze single crystals $Sr_{.60}Ba_{.40}Nb_2O_6$ have already been shown to be temperature-compensated with great promise for their device applications. Although these results are encouraging, it is important to improve the quality and properties by improving the material characteristics. This can be achieved in the present work by developing LPE layers of different compositions, and thereby obtain optimum compositions for SAW device applications. Based on our phenomenological model developed for the bronze family, the piezoelectric d_{33} and d_{15} (or e_{33} and e_{15}) and electromechanical coupling constants k_{33} and k_{15} play important roles, and their values should be large to achieve better temperature compensation in piezoelectric material. The bronze compositions based on the tetragonal solid solution $Pb_{1-x}Ba_xNb_2O_6$, $KNbO_3$-$SrNb_2O_6$ (e.g., $Sr_2KNb_5O_{15}$), etc. exhibit excellent piezoelectric characteristics and appear to be promising candidates for SAW device applications. The LPE growth of a few bronze compositions including SBN and SKN has already been initiated and has briefly been discussed in the present report.

4.1 Growth of $Sr_{.5}Ba_{.5}Nb_2O_6$ Thin Films

The LPE growth technique has successfully been developed for the bronze composition $Sr_{.5}Ba_{.5}Nb_2O_6$ by using the BaV_2O_6 solvent. The system BaV_2O_6-$Sr_{1-x}Ba_xNb_2O_6$ has been studied in great detail and, as shown in Fig. 6, the tungsten bronze SBN composition extends over a wide compositional region. At present, the composition represented along the binary join BaV_2O_6-$Sr_{.5}Ba_{.5}Nb_2O_6$ has been used for LPE growth and has proven useful for developing films of composition $Sr_{.46}Ba_{.54}Nb_2O_6$. Detailed information on this system has already been given in our earlier reports.

Table 4 summarizes the results of the LPE growth experiments for the $Sr_{.5}Ba_{.5}Nb_2O_6$ thin films grown onto the $Sr_{.6}Ba_{.4}Nb_2O_6$ substrates. The films thus grown, specifically onto the (100)- and (110)-plates, are of excellent quality and smooth. Although the surface quality is acceptable and the ferroelectric and SAW measurement work is in progress, continuous efforts are being made to improve the surface quality of the films. This task is being accomplished either by dipping the substrate at relatively higher temperatures (10°C) or by polishing the surfaces of the grown films. Both approaches seem to be suitable, and it is therefore anticipated that surface quality will not be a major problem for SAW characterization.

During the past six months, efforts were also initiated to characterize the films to examine their ferroelectric and acoustical characteristics. This requires a poled sample and has to be achieved prior to characterization. According to Ballman et al.[8], the T_c for the bronze composition $Sr_{.5}Ba_{.5}Nb_2O_6$ is around 125°C, which is substantially higher than the substrate SBN:60 (72°C). In order to obtain poled film/substrate, the sample was heated over 150°C (in oil bath) and the dc field was then applied (6 KV/cm). After sufficient time had elasped (1 hr), the sample was slowly cooled to room temperature, while the dc field was maintained. This proved to be successful, and the films were found suitable for characterization. Efforts are in progress to establish the most important parameters, such as piezoelectric coefficients d_{33}, d_{15}, e_{33} and e_{15}, and electromechanical coupling coefficients k_{33} and k_{15}; we expect these results will be available soon. Based on these measurements, it will

Table 4: EPITAXIAL GROWTH CONDITIONS FOR THE TUNGSTEN BRONZE $Sr._5Ba._5Nb_2O_6$ COMPOSITION

Composition	Solvent	Substrate Orientation	Film Thickness (μm)	Quality	Problems
$Sr._5Ba._5Nb_2O_6$	BaV_2O_6	SBN:60,(001)	20-60	Good	Slight mismatch
$Sr._5Ba._5Nb_2O_6$	BaV_2O_6	SBN:60,(100)	15-35	Excellent	None
$Sr._5Ba._5Nb_2O_6$	BaV_2O_6	SBN:60,(110)	15-35	Excellent	None
$Sr._5Ba._5Nb_2O_6$	BaB_8O_{13}	SBN:60,(001)	10-15	Moderate	Flux-problem *
$Sr._5Ba._5Nb_2O_6$	BaB_8O_{13}	SBN:60,(100)	10-215	Good	Flux-Problem

* Flux Stays on substrate after growth, however, it can be washed away in dil.Acids.

SBN:60 Corresponds to $Sr._6Ba._4Nb_2O_6$ - Composition

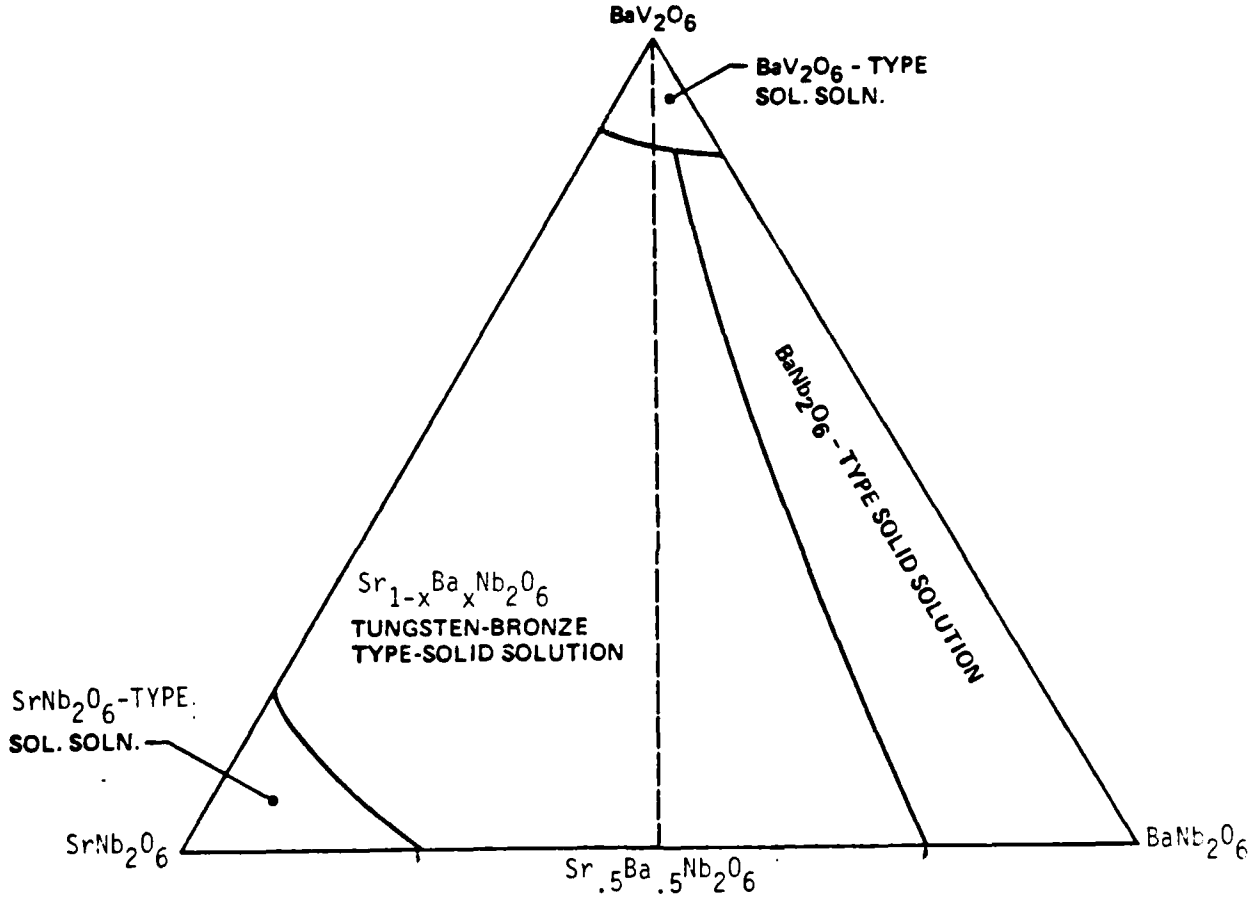

Fig. 6. The system BaV_2O_6-$SrNb_2O_6$-$BaNb_2O_6$, in air at 1200°C

be possible to anticipate temperature compensation behavior in this composition. During the next six months, SAW characteristics of this composition will also be evaluated and, based on this information, it will be possible to identify the optimum composition within the $Sr_{1-x}Ba_xNb_2O_6$, $0.25 \leq x \leq 0.75$ solid solution system.

4.2 Growth of $Sr_2KNb_5O_{15}$ Thin Films

$Sr_2KNb_5O_{15}$ (SKN) belongs to the tetragonal tungsten bronze structural family; it is ferroelectric, with Curie temperature (T_c) around 160°C. The crystal of this composition exhibits excellent dielectric, piezoelectric and electro-optic properties, which suggests possible applications for surface acoustic wave and electro-optic device applications. The single crystal growth of this composition is known and reported by various workers including the present authors. Although single crystal growth of the SKN composition is possible, the technique is confined to producing relatively small size crystals, approximately 5-6 mm in diameter. The growth of tungsten bronze compositions, in general, is difficult and success depends strongly on the ability to control the diameter of the crystal and the thermal gradient in the crystal near the solid-liquid interface. An alternative approach to this problem is LPE-grown thin films for SAW application, since the lattice mismatch between the SBN and SKN compositions is minimal and SBN single crystals of one inch in diameter are now available for such study. Table 5 summarizes physical characteristics of SBN and SKN compositions.

As identified in our earlier reports, crucial to the success of this isothermal growth is an ability to supercool the solution without occurrence of spontaneous nucleation. It is therefore necessary, before LPE can be performed, to find a suitable flux system (solvent) for the SKN composition. Based on our on-going research work in this area, a large number of solvents such as KVO_3, $K_2B_2O_4$, SrV_2O_6, SrB_8O_{13}, etc. have been identified for this composition, but the choice, at present, has been restricted to the solvent KVO_3. Since the V^{5+} cation has strong preference for the 4-fold coordinated site, the inclusion of V^{5+} in the SKN is ruled out. Further, the KVO_3 solvent melts at very low temperature (540°C) and growth should therefore be possible at low

Table 5: PHYSICAL PROPERTIES OF THE $Sr_{1-x}Ba_xNb_2O_6$ AND $Sr_2KNb_5O_{15}$ COMPOSITIONS

PHYSICAL CONSTANTS	$Sr_{.6}Ba_{.4}Nb_2O_6$	$Sr_{.5}Ba_{.5}Nb_2O_6$	$Sr_2KNb_5O_{15}$
Structural Family	Tungsten Bronze	Tungsten Bronze	Tungsten Bronze
Symmetry	Tetragonal	Tetragonal	Tetragonal
Point Group	4mm	4mm	4mm
Lattice constants	a = 12.462 Å c = 3.938 Å	12.480 Å 3.952 Å	12.470 Å 3.942 Å
Curie Temp. 0 C	72	125	156
Dielectric Constant K_{33} at room Temp.	880	500	1200
Electromechanical coupling Coefficients	K_{33} = 0.47 k_{31} = 0.14 k_{15} = 0.24	k_{33} = 0.48 k_{31} = 0.137 k_{15} = 0.---	k_{33} = 0.44 k_{31} = --- k_{15} = 0.26

temperature. The phase equilibria study for the system based on composition $K_5V_5O_{15}$-$Sr_2KNb_5O_{15}$ has been established by the DTA technique. Figure 7 shows a partial phase diagram for this system. Although it is difficult to obtain a complete phase relation for such multicomponent systems, the information obtained from this diagram is adequate to initiate the LPE growth of SKN composition.

The mixture containing 75 mole % $K_5V_5O_{15}$ and 25 mole % $Sr_2KNb_5O_{15}$ has been selected, since this mixture melts at relatively low temperatures (1000°C) and has been found to be suitable to develop thin films of the composition $Sr_2KNb_5O_{15}$. The mixture was first calcined at 650°C for about 10-15 hrs and then melted in a 100 cc platinum crucible. The crucicle was then placed in the growth furnace. As shown in Fig. 8, the growth apparatus consists of a vertical furnace which was controlled with an accuracy of ±1/2 C. The mixture was kept heated overnight at 1250°C and, after achieving complete homogeneity, the molten solution was slowly cooled to the growth temperature, around 1000°C, at the rate of 10°C/hr. The (100), (110) or (001) oriented $Sr_{.6}Ba_{.4}Nb_2O_6$ substrate, positioned slightly above the melt in order to equilibriate the solution temperature, was dipped into melt. An appropriate dipping temperature was around 1000°C. After the required time for the growth had elapsed, the sample was withdrawn from the melt and cooled very slowly to room temperature. The adhering flux was removed by dipping the substrate in dil. hydrochloric acid. The results of this investigation are similar to those observed for the growth of $Sr_{.5}Ba_{.5}Nb_2O_6$ composition on SBN substrate. In the present case, the growth was also much faster on the (001) plate, compared to the other orientations. This is consistent with our observations on the bulk single crystal growth of the $Sr_2KNb_5O_{15}$ composition, where growth was only possible along the (001) direction. Figure 9 shows a typical cross-section of the SKN film grown onto the (001) plane; thickness of the film is approximately 20 μm. By using this technique, it was possible to grow films as thick as 25-30 μm, which is a significant accomplishment in the present work.

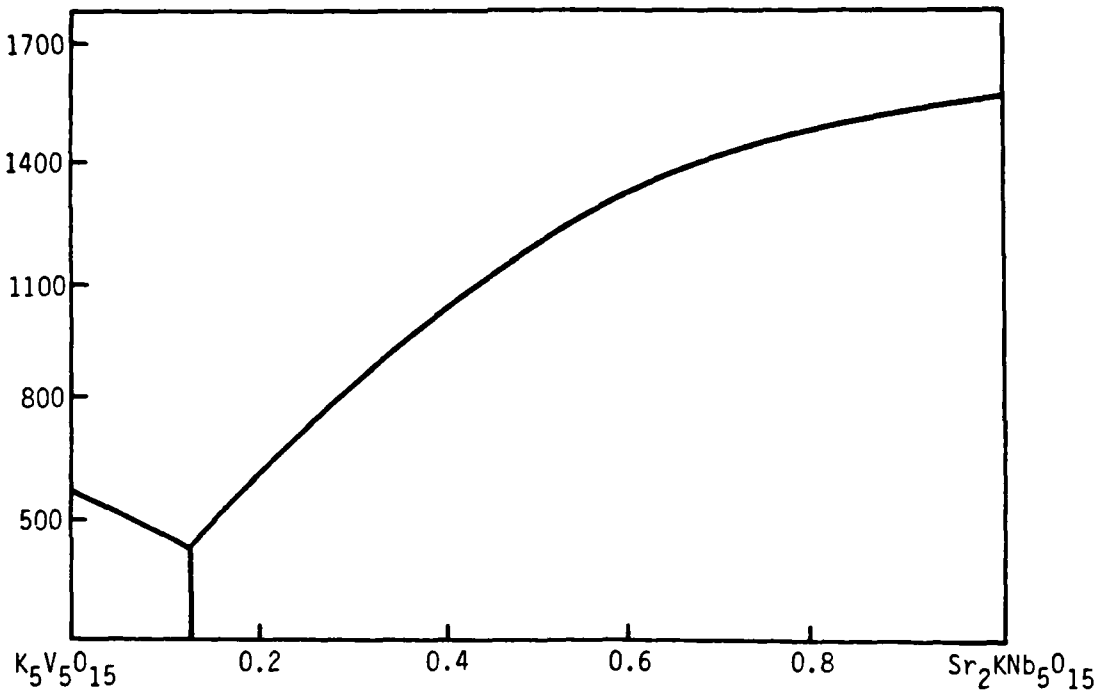

Fig. 7. Pseudo-binary phase diagram for the $K_5V_5O_{15}$-$Sr_2KNb_5O_{15}$ system.

MRDC81-15547

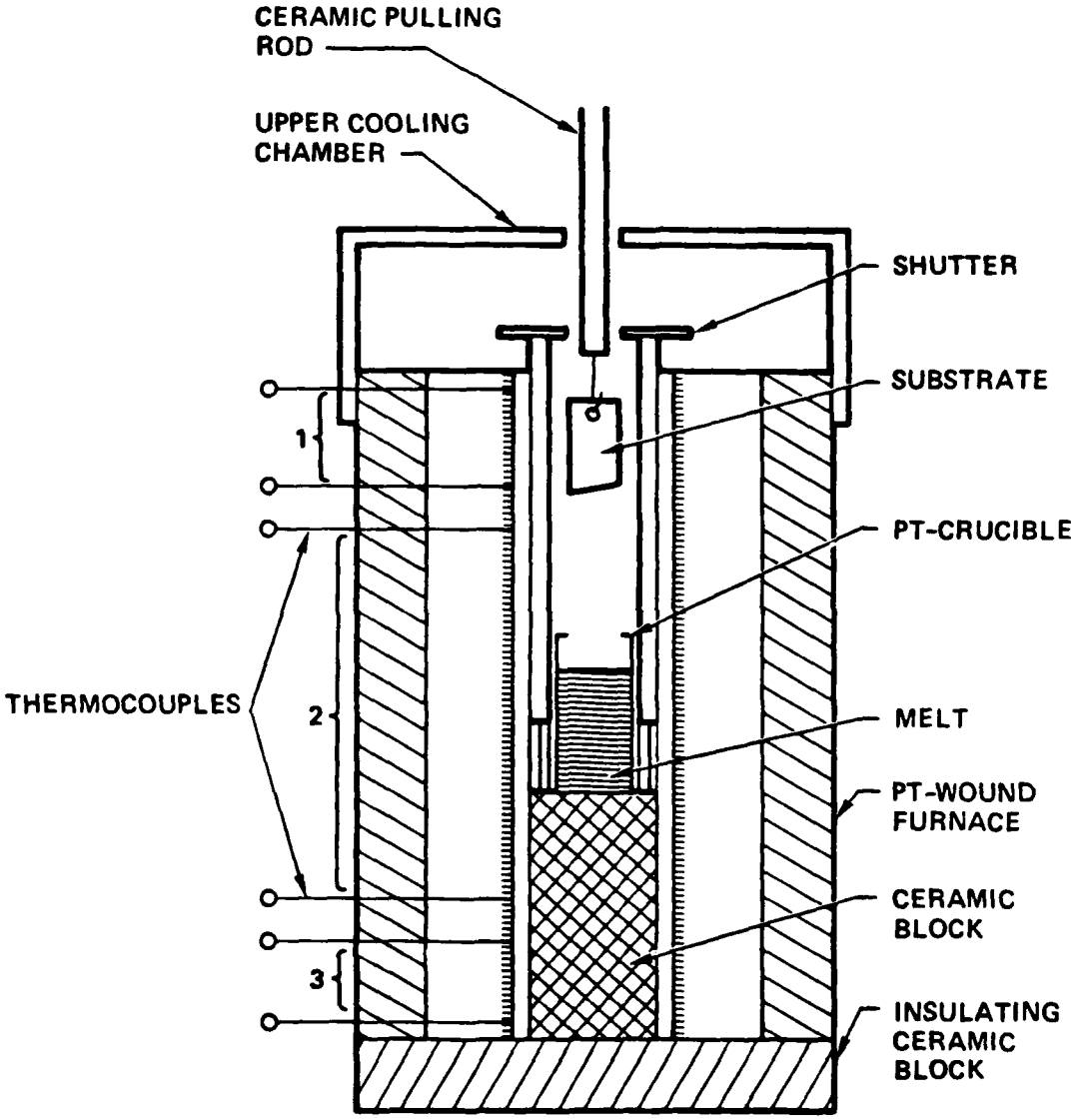

Fig. 8. LPE thin film growth furnace.

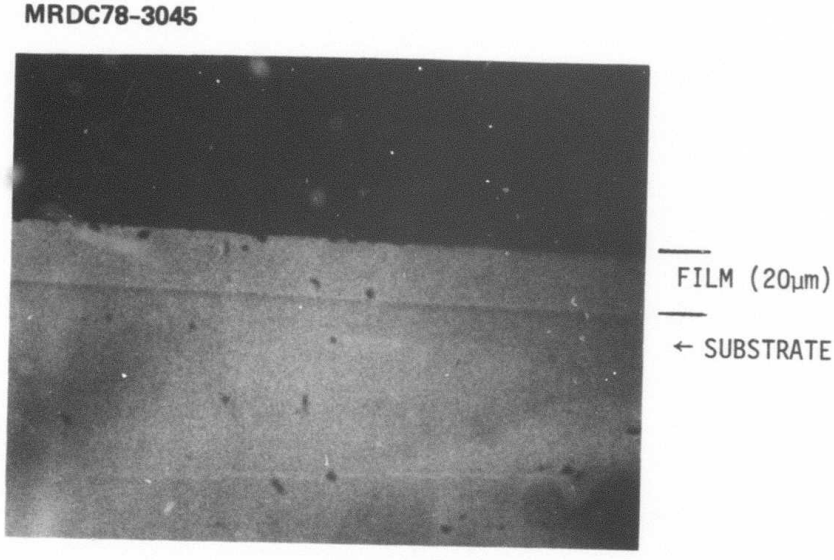

Fig. 9 A typical cross-section of the $Sr_2KNb_5O_{15}$ film on the (001)-cut SBN:60 substrate.

The films grown from KVO_3 flux are dark amber to yellow in color, depending on the film thickness, and the surface is smooth and clear. Microscopic examination at high magnification showed a slightly rougher aspect in the case of thicker films, in range 30-35 μm films. The crystallinity and film growth have been established by the X-ray diffraction technique. A typical intensity vs. film thickness plot is given for the reflection (002) in Fig. 10. Two peaks corresponding to CuK α_1 and K α_2 represent the $Sr_{.6}Ba_{.4}Nb_2O_6$ substrates, while the SKN film position is denoted by CuK' α_1 and K' α_2. The intensity of film reflection was significantly stronger than that of the substrate, indicating the high degree of crystallinity as well as confirmation of the growth of SKN layer on the SBN substrate. The lattice constants determination for substrate/film is in progress to establish the film composition, i.e., the ratio Sr:K in the composition $Sr_2KNb_5O_{15}$.

Recently Adachi et al.[9] also demonstrated the successful heteroepitaxial growth of another bronze composition $K_3Li_2Nb_5O_{15}$ on the bronze $K_2BiNb_5O_{15}$ substrate material by the rf sputtering and LPE techniques. The $K_3Li_2Nb_5O_{15}$ films thus grown were shown to be of excellent quality and thickness was approximately 3-4 μm. Although this work is similar to our present work, the growth rate of the SKN composition is much faster and we have successfully grown SKN films as thick as 25-30 μm. The quality of our films is excellent, which is considered a major accomplishment in the present work. Further work on the SKN films is in progress to improve the film quality and a few other details; however, this opens a new interest for this family and their applications not only for SAW devices, but also in other areas such as electro-optics, acousto-optics and non-linear optics. As summarized in Table 6, there are a number of other important bronze compositions that possess excellent dielectric, piezoelectric, and optical properties, but these are extremely difficult to grow in the form of bulk single crystals. Since the lattice mismatch between the selected compositions and the substrate materials such as $Sr_{1-x}Ba_xNb_2O_6$, x = 0.50 and 0.60, and $Ba_{1.2}Sr_{.8}Na_{.25}K_{.75}Nb_5O_{15}$ is minimal, it will be possible to develop some of these compositions for a wide variety of applications. Work on a few compositions is already in progress, and it will be possible to characterize them in the next six months.

SC79-4451

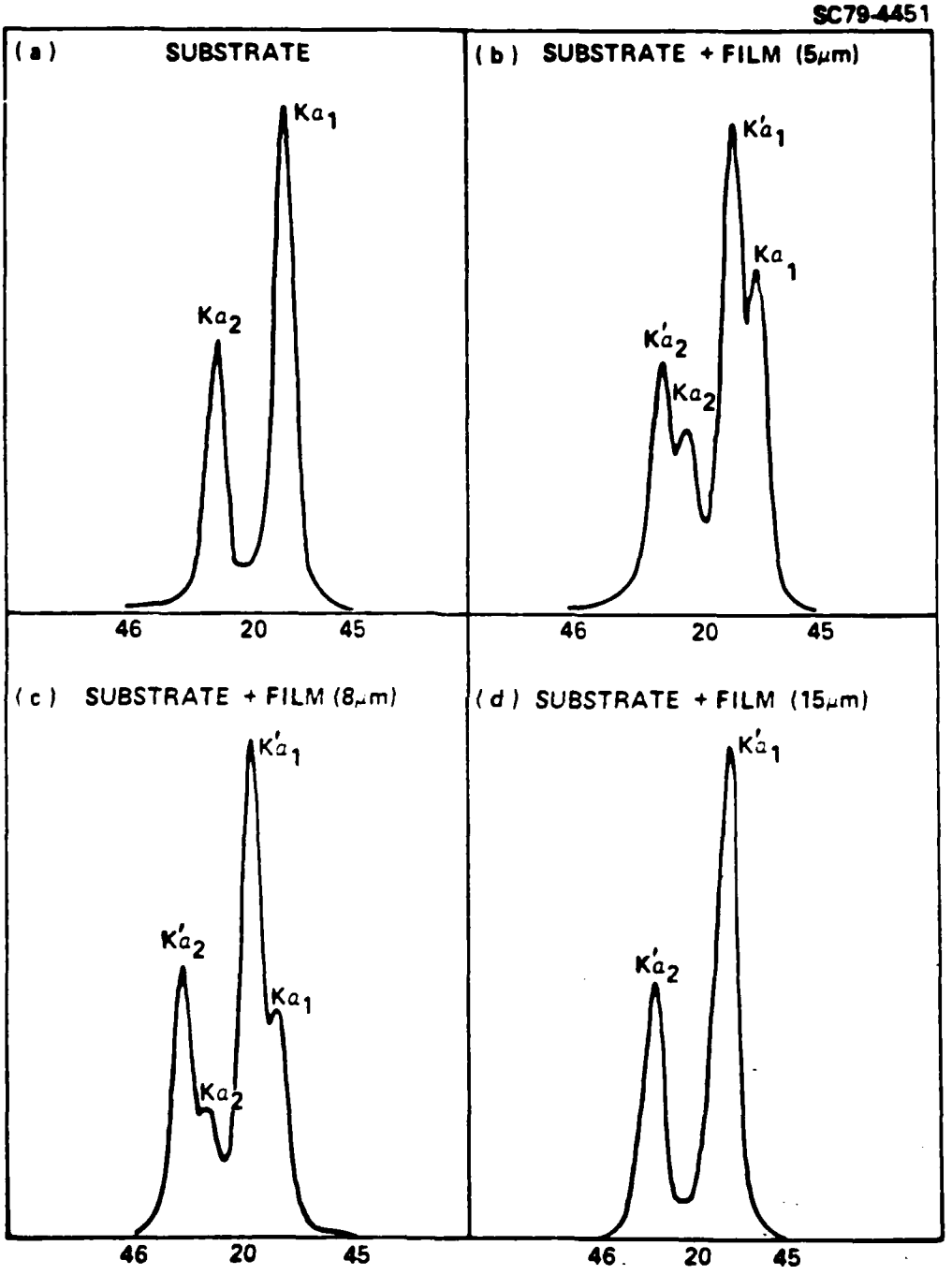

Fig. 10. X-ray diffraction peak taken for substrate/film.

Table 6. Selected Bronze Compositions for Epitaxial Growth.

COMPOSITION	SOLVENT	MELTING TEMP. (°C)	SUPERCOOLING* RANGE (°C)	CRYSTALLIZATION RANGE	LATTICE CONSTANTS a_A	LATTICE CONSTANTS c_A
$Sr_{1-x}Ba_xNb_2O_6$**	BaV_2O_6 SrV_2O_6	700 740	40-60 40	Long and useful Short and useful	12.435 to 12.495	3.923 to 3.975
$Sr_2KNb_5O_{15}$	KVO_3	540	30-40	Long and useful	12.473	3.942
$Ba_2Na_3YNb_{10}O_{30}$	BaV_2O_6	700	---	Long and useful	12.440	3.933
$Ba_{2-x}Sr_xK_{1-y}Na_yNb_5O_{15}$	KVO_3 $NaVO_3$	540 650	--- ---	----- -----	12.483	3.955
$Ba_2SrTiNb_4O_{15}$	BaV_2O_6	700	---	Long and useful	12.445	3.940
$Ba_2K_{1-y}Na_yNb_5O_{15}$	KVO_3	540	---	-----		
$Pb_{1-x}Ba_xNb_2O_6$	$Pb_2V_2O_7$	680	---	Useful	12.472	3.955

* Supercooling range for these systems was established by the DTA technique.

**Lattice constants are given for the tetragonal tungsten bronze solid solution.

5.0 STRUCTURAL AND FERROELECTRIC PROPERTIES OF THE PHASE $Pb_{1-2x}K_xM^{3+}_xNb_2O_6$, M = La OR Bi

5.1 Introduction

Lead metaniobate, $PbNb_2O_6$, was first studied and reported ferroelectric by Goodman in 1953[10-11]; since then, this material has been the subject of several investigations[12-23]. Although the Curie temperature was much higher than that of any known ferroelectric, the material did not find immediate application because of the difficulty in preparing good non-porous ceramic and the associated problem of poling them. By analogy with previous work on barium titanate and other ferroelectric hosts, the effect of replacing part of the Pb^{2+} by other divalent and trivalent ions[24-27] or Nb^{5+} by tetravalent or hexavalent ions was studied, with the objective of improving the sintering and general ferroelectric properties of ceramics. It was reported that the Curie temperature was reduced and, although this would be a disadvantage, this made it possible to pole the material more effectively and to successfully enhance the dielectric and piezoelectric properties.

Since our current interest is in surface acoustic wave and millimeter wave device applications, the search for a suitable ferroelectric material having high dielectric and piezoelectric properties is constantly being made. The present work reports the structural, dielectric and piezoelectric properties of the solid solutions based on the $PbNb_2O_6$ phase, e.g., $Pb_{1-2x}K_xM^{3+}_xNb_2O_6$, where M = La or Bi.

5.2 Experimental Procedure

PbO, K_2CO_3 (Baker Analyzed Grade), Bi_2O_3 (Fischer Scientific Co,), La_2O_3 (American Potash and Chem. Corp.), and Nb_2O_5 (Atomergic Co.) were used as the starting materials. The ceramic specimens were prepared by the conventional technique of milling, prefiring, crushing, pressing and firing. The specimens were prepared in the form of disks 1.3 cm in diameter and 0.3 cm

thick. The final sintering was for 2-3 hours, and the temperature, which depended on composition, was between 1250°-1300°C.

Preparation of pure $PbNb_2O_6$ is complicated by the existence of ferroelectric and non-ferroelectric modifications[10]. The transition between these modifications is reversible, although it is accompanied by considerable temperature hysteresis. The high-temperature ferroelectric form was prepared by heating to 1320°C for 30 minutes and then cooling rapidly[11]. X-ray powder diffraction data were obtained with a Norelco diffractometer, using CuK radiation and a graphite monochromator operating at 35 kV and 28 ma. Measurements were made from strip charts, produced by scanning ¼ 2Θ/min on acetone smear-mounted powders. The measurements are believed to be accurate to ±0.02 2Θ. Instrumental error was corrected through the use of an internal silicon standard. Least-squares analysis of the data for refined cell constants was performed on a Harris Model 1660 computer.

The fired disks were metallized on the major surfaces by using either platinum paste or a vacuum-deposited layer of platinum. Disks required to be poled were heated in silicon oil, and a static field of 20 kV per cm was applied at temperatures as near as possible to 150 to 170°C, the field being maintained while the disks were allowed to cool.

5.3 Crystalline Solubility and Structural Transitions

The work on $K_{.5}La_{.5}Nb_2O_6$ by Soboleve et al.[27-28] and our work on $K_{.5}Bi_{.5}Nb_2O_6$[29] show that these two phases crystallize in the tetragonal crystal symmetry and are isostructural with high temperature tetragonal modification of $PbTa_2O_6$. At room temperature, the ferroelectric $PbTa_2O_6$ phase has an orthorhombic symmetry and is isostructural with the tungsten bronze $PbNb_2O_6$ phase. This suggests that all the systems considered in this work are structurally related and should form a continuous solid solution on the pseudo-binary systems, $PbNb_2O_6$-$K_{.5}La_{.5}Nb_2O_6$ and $PbNb_2O_6$-$K_{.5}Bi_{.5}Nb_2O_6$. The results of X-ray diffraction powder work are in good agreement, and a complete solid solution has been identified on both the systems. Three structurally related phases, namely the orthorhombic and the tetragonal tungsten bronze type phases

and the tetragonal $K_{.5}La_{.5}Nb_2O_6$ have been established for the $Pb_{1-2x}K_xM^{3+}_xNb_2O_6$, M = La or Bi, solid solution system. Figure 11 shows X-ray diffraction powder patterns for the three phases.

The results of X-ray measurements, at room temperature, show a homogeneity range of the orthorhombic tungsten bronze phase to x = 0.50, while the tetragonal tungsten bronze phase is present in the composition range $0.50 \leqslant x \leqslant 0.85$. At the other end, the crystalline solid solubility of $PbNb_2O_6$ in the $K_{.5}M^{3+}_{.5}Nb_2O_6$ phase is limited and is estimated to be in the composition range $0.86 \leqslant x \leqslant 1.0$. At composition x = 0.50, both the orthorhombic and tetragonal tungsten bronze phases coexist. This type of morphotropic condition has also been reported on the $Pb_{1-x}Ba_xNb_2O_6$ system[20-21]. The variation of lattice parameters as a function of composition for the system $Pb_{1-2x}K_xLa_xNb_2O_6$ has been shown in Fig. 12. The a and c parameters increased only slightly, while the b parameter decreased considerably with increasing concentration of $K_{.5}M^{3+}_{.5}Nb_2O_6$ in the $PbNb_2O_6$ phase. The decrease in the b parameter was substantial compared to the a parameter, so that the ratio b/a becomes close to unity for values $x \geqslant 0.50$.

5.4 Ferroelectric Data

The Curie temperature, T_c, is known to be one of the fundamental characteristics of ferro- and anti-ferroelectrics. This measurement gives the origin of the spontaneous polarized state and is considered important for characterizing the piezoelectric materials. In the present work, T_c for the different solid solution systems has been obtained by measuring the dielectric properties as a function of temperature. The technique is relatively simple, and the measurements have been routinely made by using a capacitance bridge (HP 4270A). The test specimens (disks) used for the dielectric measurements are approximately 1.3 cm in diameter and 0.3 cm thick, and are coated on each side with platinum by the standard vacuum evaporation technique.

A typical plot of the dielectric constant vs. temperature is given in Fig. 13 for a few compositions on the $Pb_{1-2x}K_xLa_xNb_2O_6$ systems. It can be seen that the peak at Curie temperature is sharp and is shifted toward a

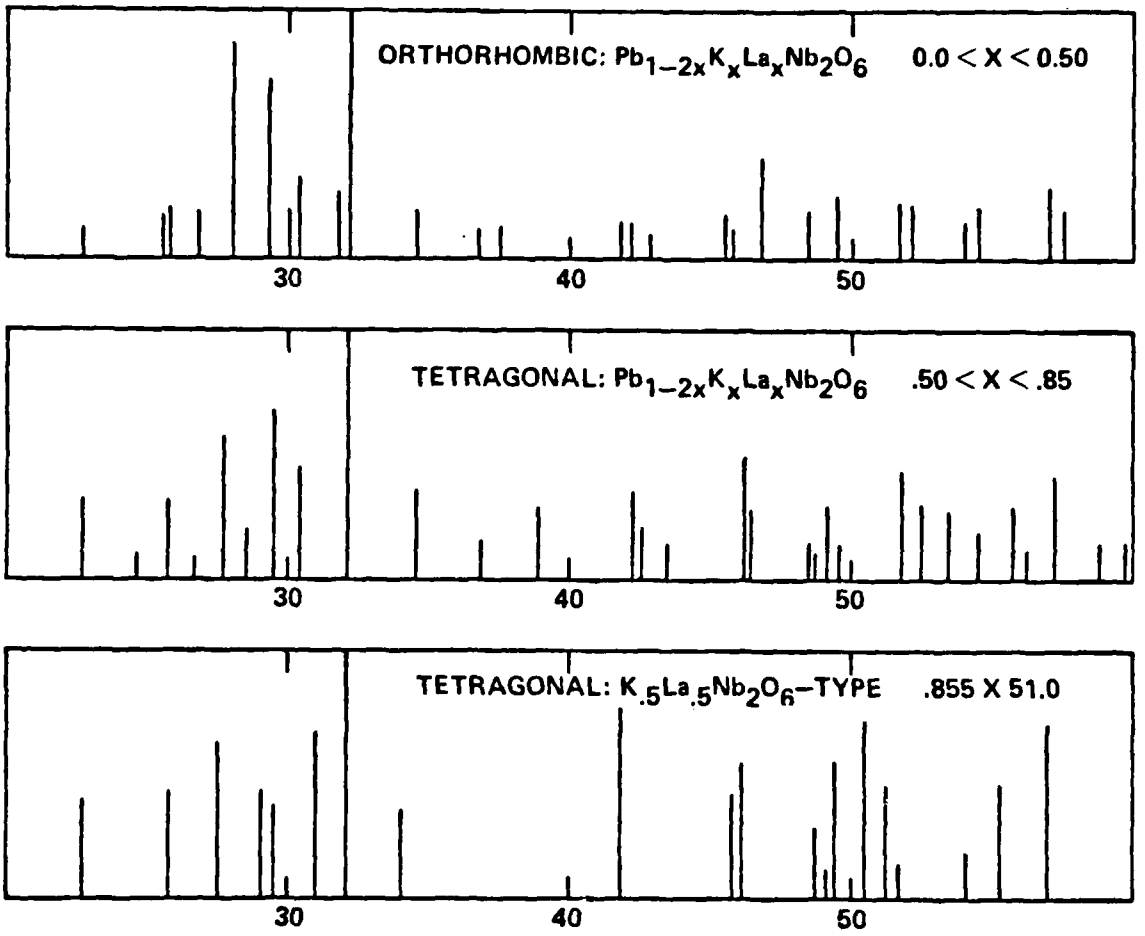

Fig. 11. X-ray powder diffraction patterns for the $Pb_{1-2x}K_xLa_xNb_2O_6$ solid solution system.

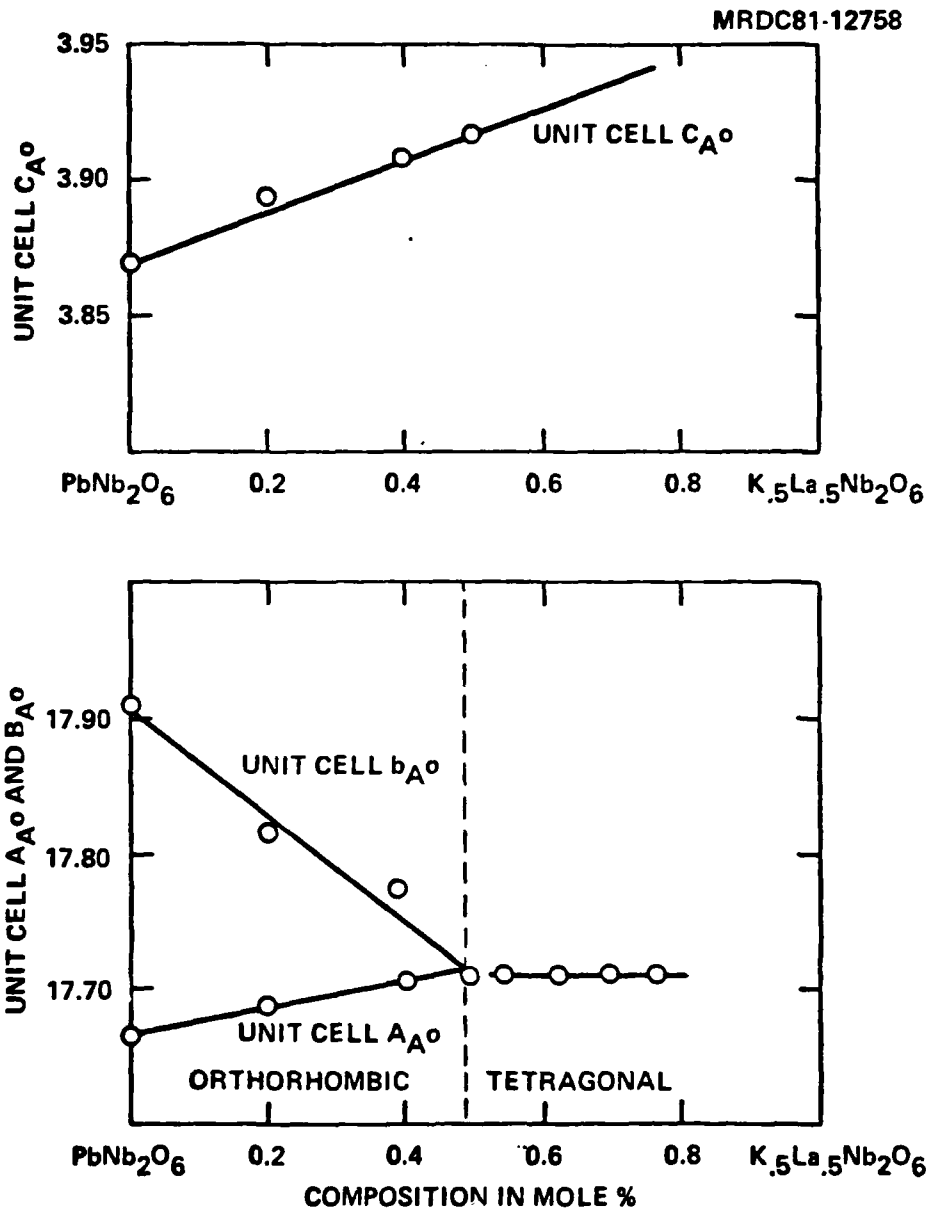

Fig. 12. Variation of lattice parameters for the $Pb_{1-2x}K_xM^{3+}_xNb_2O_6$, M = La or Bi.

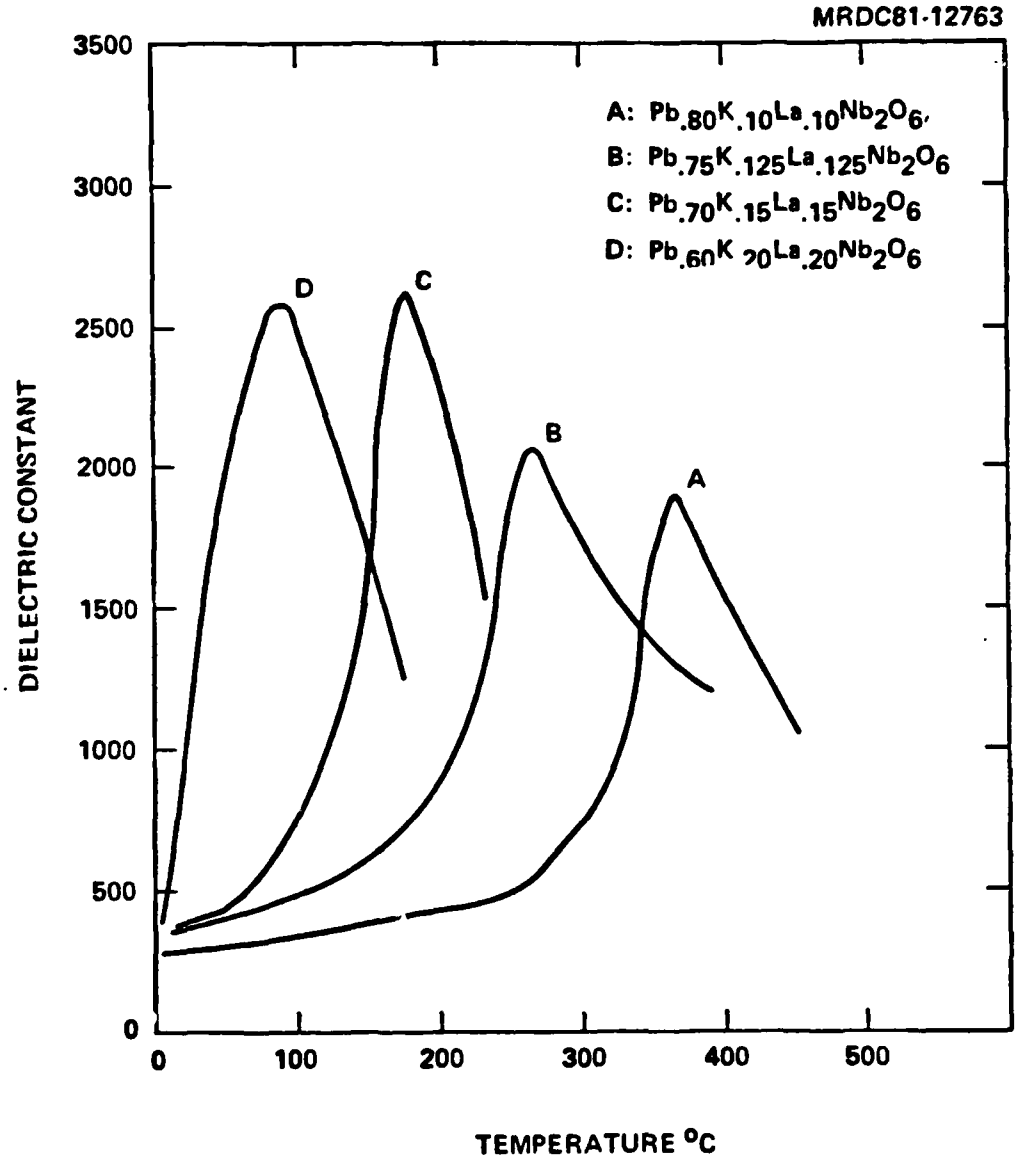

Fig. 13. Variation of the ferroelectric T_c as a function of composition for the $Pb_{1-2x}K_xLa_xNb_2O_6$.

lower temperature with increasing amounts of $K_{.5}La_{.5}Nb_2O_6$ in $PbNb_2O_6$. T_c for the pure $PbNb_2O_6$ has been recorded at 560°C, and this temperature dropped for all the additions of K^+ and La^{3+} or Bi^{3+} in both the orthorhombic and the tetragonal tungsten bronze phases. By using this peak position, the transition temperature for each system has been determined. Figure 14 shows the variation of T_c as a function of composition for the $Pb_{1-2x}K_xLa_xNb_2O_6$ and $Pb_{1-2x}K_xBi_xNb_2O_6$ systems. Variation of T_c with composition is linear in both systems and is approximately of the same order. Lowering of the T_c has also been reported for several other systems based on the $PbNb_2O_6$ solid solutions[12-25].

The effect of variety of different substituent ions, such as Ba^{2+}, Sr^{2+}, Ca^{2+}, Cd^{2+} and Bi^{3+} for Pb^{2+} in the $PbNb_2O_6$ phase, has been studied and reported in literature[13-19]. Except for Ba^{2+}, all other ions are smaller than Pb^{2+}, and their addition did not alter the orthorhombic crystal symmetry. However, in the case of the $Pb_{1-x}Ba_xNb_2O_6$ solid solution system[20-21], the substitution of Ba^{2+} (150Å) for Pb^{2+} (132Å) first decreases the orthorhombic distortion, and then induces a tetragonal structure with polar axis along the c rather than along the b axis. Further, the interesting feature in this system is that T_c first decreased in the orthorhombic tungsten bronze phase and then increased in the tetragonal tungsten bronze phase. This is the unique case in the $PbNb_2O_6$-based solid solutions; also, since the average ionic size of $K^+ + La^{3+}$ (1.355Å) and $K^+ + Bi^{3+}$ (1.34Å) is bigger than Pb^{2+} and since both systems, e.g., $Pb_{1-2x}K_xM^{3+}_xNb_2O_6$, M = La or Bi, and $Pb_{1-x}Ba_xNb_2O_6$, are structurally similar, it was expected that the addition of K^+ with La^{3+} or Bi^{3+} would produce similar results, i.e., first a decrease and then an increase in the T_c. The results of this investigation (Fig. 14) indicate that the continuously decreasing Curie temperature occurs with increasing amounts of $K^+ + La^{3+}$ or $K^+ + Bi^{3+}$ in both the orthorhombic and tetragonal tungsten bronze phases, indicating that T_c is not only controlled by the size of substituent ions, but its location in the structure is equally important. Since the coordination of Pb^{2+} is 15- and 12- fold in the tungsten bronze structure, there exist three possibilities for each ion in this structure, namely in the 15 or 12, or in both the sites. Neither the work reported in the literature[12-24] nor the results of this investigation are sufficient to establish the site

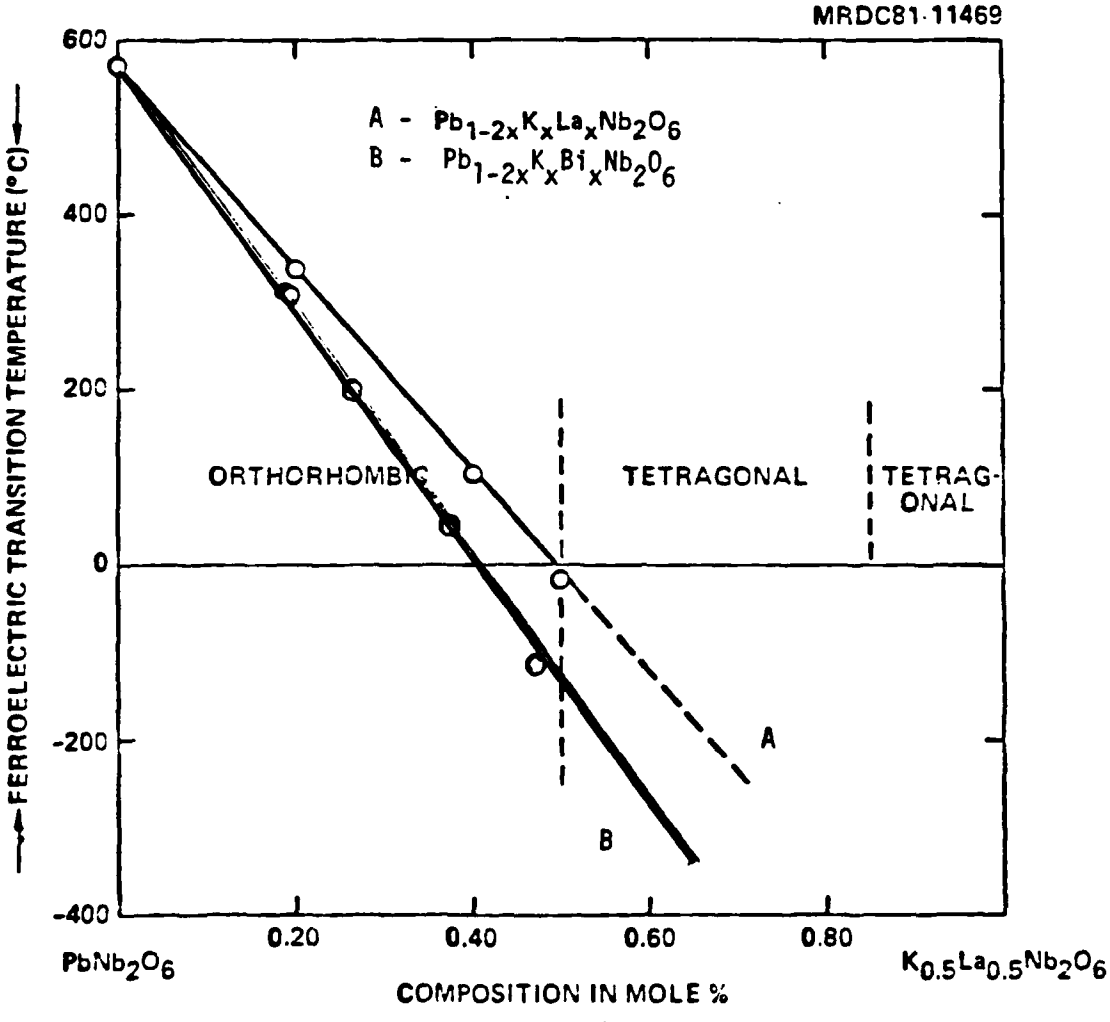

Fig. 14. Variation of the ferroelectric T_c for the $Pb_{1-2x}K_xM^{3+}_xNb_2O_6$, M = La or Bi.

preference or their distribution over the two crystallographic sites. Further work in this direction is of significant interest in the present study in order to establish the site preference for different ions and their influence over the T_c behavior, and ferroelectric properties.

6.0 FUTURE PLANS

6.1 Application of Phenomenological Model

Based on the phenomenological analysis on the tungsten bronze family, it has been shown that the sixth order electrostriction constants Φ_{ijklmn} play an important role in studying the elastic behavior in the single domain ferroelectric phase. This work will be continued to obtain more information on the tungsten bronze family compositions such as $Pb_{1-x}Ba_xNb_2O_6$ and $Ba_{2-x}Sr_xK_{1-y}Na_yNb_5O_{15}$.

6.2 Piezoelastic Measurements

All of the piezoelastic tensor elements of the material SBN:61 have been evaluated using appropriate resonator geometries. For future work, it has been planned that more detailed studies be conducted with the 2nd order coefficients with respect to temperature over the range -20 to +50°C. In addition, the stability of the SBN crystals at a constant temperature will be evaluated. Based on this extensive work, changes in composition or in growth technique may be undertaken.

6.3 Materials Preparation and Acoustical Characterization

The liquid phase epitaxial (LPE) technique has been shown to be successful for developing the bronze compositions $Sr_{.5}Ba_{.5}Nb_2O_6$ and $Sr_2KNb_5O_{15}$ onto various crystallographic orientations such as (100), (110) and (001) of $Sr_{.6}Ba_{.4}Nb_2O_6$ substrates. The poling technique for the compositions $Sr_{.5}Ba_{.5}Nb_2O_6$ has been established and this should make possible the determination of the ferroelectric and acoustical properties of the films. Once the acoustical properties for these films are determined, efforts will be made to modify the film composition to obtain optimum SAW composition. During the next six months, efforts will also be made to evaluate and characterize $Sr_2KNb_5O_{15}$ and other important bronze films that possess excellent piezoelectric

e_{15} or d_{15} and electromechanical coupling coefficient k_{15}.

6.4 Electro-Optic Measurements

Optical measurements will be continued to determine the half-wave voltage for the different boules of $Sr_{.61}Ba_{.39}Nb_2O_6$ single crystals. Once this task is accomplished, efforts to grow optical quality SBN single crystals will be made.

7.0 PUBLICATIONS AND PRESENTATIONS

7.1 Publications

1. R. R. Neurgaonkar, T. C. Lim, E. J. Staples and L. E. Cross, "An Exploration of the Limits of Stability of the $LiNbO_3$ Structure Field with A and B Site Cation Substitutions", Ferroelectrics 27-28, 63 (1980).

2. K. L. Keester, R. R. Neurgaonkar, T. C. Lim and E. J. Staples, "Strontium Metaniobates: Its Crystallography, Polimorphism and Isomorphism", Mat. Res. Bul. 15, 821 (1980).

3. R. R. Neurgaonkar, M. H. Kalisher, T. C. Lim, E. J. Staples and K. L. Keester, "Czochralski Single Crystal Growth of $Sr_{.61}Ba_{.39}Nb_2O_6$ for Surface Acoustic Wave Devices", Mat. Res. Bull. 15, 1235 (1980).

4. L. E. Cross, R. Betch, H. McKinstry, T. Shrout and R. R. Neurgaonkar, "A New Method for Predicting the Temperature Dependence of Elastic Compliance in Simple Proper Ferroelectrics", Proceedings of Frequency Control Symposium, 25-33 (1980).

5. R. R. Neurgaonkar and W. K. Cory, "Structural and Dielectric Properties of $Ba_6Ti_2Nb_8O_{30}$-Type Tungsten Bronze Compositions", (in preparation).

6. R. R. Neurgaonkar, T. C. Lim, E. J. Staples and L. E. Cross, "Crystal Chemistry of Ferroelectric Materials for SAW Devices", Proceedings of Ultrasonic, 410 (1980).

7. T. R. Shrout, L. E. Cross, P. Moses, H. A. McKinstry and R. R. Neurgaonkar, "A Phenomenological Theory for Predicting the Temperature Dependence of Elastic, Dielectric and Piezoelectric Properties in Simple Proper Ferroelectric Crystals", Proceedings of Ultrasonics, 414 (1980).

8. R. R. Neurgaonkar, W. K. Cory and L. E. Cross, "Structural and Ferroelectric Properties of the Phase $Pb_{1-2x}K_xM^{3+}_xNb_2O_6$, M = La or Bi", submitted to Mat. Res. Bull.

9. R. R. Neurgaonkar, W. K. Cory, W. W. Ho, W. F. Hall and L. E. Cross, "Tungsten Bronze Family Crystals for Acoustical and Dielectric Applications", Ferroelectrics 38, 857 (1981).

10. E. J. Staples and R. R. Neurgaonkar, "SAW Transduction and Poling in Ferroelectric Strontium Barium Niobate", Ferroelectrics 38. 882 (1981).

11. T. R. Shrout, L. E. Cross, P. Moses, H. A. McKinstry and R. R. Neurgaonkar, "Higher Order Electrostriction in Ferroelectric Tungsten Bronzes", Ferroelectrics 38, 881 (1981).

12. W. Ho, W. F. Hall, R. R. Neurgaonkar, R. E. DeWames and T. C. Lim, "Microwave Dielectric Properties of $Sr_{.61}Ba_{.39}Nb_2O_6$ Single Crystals", Ferroelectrics 38, 833 (1981).

7.3 Presentations

1. R. R. Neurgaonkar, T. C. Lim, E. J. Staples and L. E. Cross, "An Exploration of the Limits of Stability of the $LiNbO_3$ Structural Field with A and B Site Cation Substitutions", Presented at the IEEE Int. Symposium of Ferroelectrics, Minneapolis, MN, June 13-15, 1979.

2. K. L. Keester, R. R. Neurgaonkar, T. C. Lim and E. J. Staples, "Conoscopic Characterization of Czochralski Grown Strontium-Barium Niobate Boules", Presented at the 4th Conference on Crystal Growth, Stanford Sierra Camp, Fallen Leaf, California, May 16-18, 1979.

3. L. E. Cross, R. Betch, H. McKinstry, T. Shrout and R. R. Neurgaonkar, "A New Method for Predicting the Temperature Dependence of Elastic Compliance in Simple Proper Ferroelectrics", Presented at the 34th Annual Symposium on Frequency Control, Philadelphia, PA, May 28-30, 1980.

4. R. R. Neurgaonkar, T. C. Lim, E. J. Staples and L. E. Cross, "Crystal Chemistry of Ferroelectric Materials for SAW Devices", Presented at the Annual Ultrasonic Symposium, Boston, MA, Nov. 1980.

5. T. R. Shrout, L. E. Cross, P. Moses, H. A. McKinstry and R. R. Neurgaonkar, "A Phenomenological Theory for Predicting the Temperature Dependence of Elastic, Dielectric and Piezoelectric Properties in Simple Proper Ferroelectric Crystals", presented at the Annual Ultrasonic Symposium, Boston, MA, Nov. 1980.

6. R. R. Neurgaonkar, W. K. Cory, W. W. Ho, W. F. Hall and L. E. Cross, "Tungsten Bronze Family Crystals for Acoustical and Dielectric Applications", presented at the 5th International Meeting on Ferroelectricity, State College, PA, August 17-21, 1981.

7. R. R. Neurgaonkar, W. K. Cory, T. C. Lim and L. E. Cross, "Solid Solution Based on Ferroelectric $Pb_{1-2x}K_xLa_xNb_2O_6$", Presented at the 83rd Annual Conference of American Ceramic Society, Washington, D.C., May 4-6, 1981.

8. E. J. Staples and R. R. Neurgaonkar, "SAW Transduction and Poling in Ferroelectric Strontium Barium Niobate" Presented at the 5th International Meeting on Ferroelectricity, State College, PA, August 17-21, 1981.

9. T. R. Shrout, L. E. Cross, P. Moses, H. A. McKinstry and R. R. Neurgaonkar, "Higher Order Electrostriction in Ferroelectric Tungsten Bronzes" Presented at the 5th International Meeting on Ferroelectricity, State College, PA, August 17-21, 1981.

REFERENCES

1. N. Uchica and N. Niizeki, Proc. IEEE 61, 1073 (1973).

2. P. H. Carr, Proceedings of Ultrasonic Symposium, 286 (1974).

3. R. Whatmore, J. Cryst. Growth 48, 530 (1980).

4. T. Yamada, J. Appl. Phys. 41, 4141 (1970).

5. R. R. Neurgaonkar, Annual Technical Report No. 2, Contract No. F49620-78-C-0093, 1981.

6. M. Adachi and A. Kawabata, Jap. J. Appl. Phys. 17, 1969 (1978).

7. L. E. Cross, private communication.

8. A. A. Ballman and H. Brown, J. Cryst. Growth 1, 311 (1967).

9. M. Adachi, T. Shiosaki and A. Kawabata, Jap. J. Appl. Phys. 18, 193 (1979).

10. G. Goodman, J. Am. Ceram. Soc. 36, 368 (1953).

11. G. Goodman, Am. Ceram. Bull. 31, 113 (1952).

12. G. A. Smolenskii and A. I. Agranovskyaya, Dokl. Akad. Nauk. SSSR 97, 237 (1954).

13. R. V. Coates and H. F. Kay, Phil. Mag. 8, 1449 (1958).

14. E. C. Subbarao, J. Am. Ceram. Soc. 43, 439 (1960).

15. E. C. Subbarao, G. Shirane and F. Jona, Acta. Cryst. 13, 226 (1960).

16. E. C. Subbarao, J. Am. Ceram. Soc. 44, 92 (1961).

17. S. Srikanta, V. B. Tare, A. P. B. Sinha and A. B. Biswas, Acta. Cryst. 15, 255 (1962).

18. E. C. Subbarao and J. Hrizo, J. Am. Ceram. Soc. 45, 528 (1962).

19. P. Baxter and N. J. Hellicar, J. Am. Ceram. Soc. 43, 578 (1960).

20. M. H. Francombe and B. Lewis, Act. Cryst. 11, 696 (1958).

REFERENCES (Cont.)

21. M. H. Francombe, Acta. Cryst. 13, 131 (1960).

22. V. A. Isupov, V. I. Kosiakov, Zh. Tekh. Fiz. 28, 2175 (1958).

23. E. G. Bonnikova, I. M. Larionov, N. D. Smazhevskaya and E. G. Glozman, Izv. Akad. Nauk. SSSR, Ser. Fiz. 24, 1440 (1960).

24. E. G. Smazhevskaya and V. I. Rivkin, Izv. Akada. Nauk. SSSR, Ser. Fiz. 24, 1398 (1960).

25. G. Goodman, Am. Ceram. Soc. Bull. 34, No. 4, Program 11; U.S. Patent No. 2,805,165, September 3, 1957, filed April 25, 1955.

26. E. C. Subbarao and G. Shirane, J. Chem. Phys. 32, 1846 (1960).

27. L. V. Soboleva and F. I. Dmitrieva, Inorg. Mat. 6, 1761 (1970).

28. M. H. Francombe, Acta. Cryst. 9, 683 (1956).

29. R. R. Neurgaonkar and L. E. Cross, private communication.